

CAUSALAB: A SCALABLE ENVIRONMENT FOR INTERACTIVE CAUSAL DISCOVERY TOWARD AI SCIENTISTS

Junlin Yang^{*1}, Dylan Zhang^{*2}, Xiangchen Song³, Qirun Dai⁴, Xiao Liu⁴, Yuen Chen², Aniket Vashishtha², Jing Shi⁵, Chenhao Tan⁴ and Hao Peng²

¹Tsinghua University, ²University of Illinois Urbana-Champaign, ³Carnegie Mellon University, ⁴University of Chicago, ⁵Adobe

We introduce *CausaLab*, a scalable environment for evaluating interactive causal discovery by LLM agents. Unlike prior evaluations, *CausaLab* evaluates both whether an agent can solve a problem using causal evidence and whether its answer is supported by a correct hypothesis about the underlying causal mechanism. Each episode places an agent in a synthetic laboratory: it receives prior measurement records, intervenes on a manipulator crystal, and predicts the resonance frequency of a held-out reactor crystal governed by the same mechanism. The hidden data-generating process is a randomly sampled structural causal model (SCM), so success requires recovering both a causal graph and structural equations rather than recalling prior knowledge. *CausaLab* also includes a domain-specific language that records the agent’s evolving SCM hypothesis, making trajectories inspectable and comparable with ground truth. Experiments show a persistent gap between prediction and mechanism recovery: in the purely observational 6-node setting, GPT-5.2-high reaches 92% task accuracy but only 0.471 all-edge F_1 . This observation further motivates our exploration of different interaction strategies: Mixed observation–intervention strategies improve structural fidelity: in the mixed 6-node setting, GPT-5.2-high achieves 80% on both task accuracy and all-edge F_1 . Yet even strong agents struggle to design informative interventions, as pure intervention strategies perform poorly on both task accuracy and all-edge F_1 . We identify premature stopping as a major weakness of agents, and show that asking the model to verify the consistency between its hypothesis and past data can help mitigate this issue. *CausaLab* therefore separates predictive success from causal understanding and exposes current LLM agents’ limits as experimental causal reasoners.

Code: <https://github.com/DylanZSZ/CausaLab>

*Junlin Yang and Dylan Zhang contributed equally and both serve as project leads. Junlin Yang’s work was done at the University of Illinois Urbana-Champaign.

1. Introduction

Causal reasoning is important because scientific, medical, and policy decisions depend on how systems would respond to interventions, not only on observed associations (Pearl, 2009; Pearl and Mackenzie, 2018; Imbens and Rubin, 2015). Yet measuring and making progress in causal reasoning remains challenging, particularly for today’s large language models (LLMs). Existing benchmarks generally translate causal graphs, datasets, or narratives into question-answering and classification tasks (Qin et al., 2019; Romanou et al., 2023; Stolfo et al., 2023; Jiang et al., 2024; Vashishtha et al., 2025; Jin et al., 2023a; Wang, 2024; Chen et al., 2024b; Jin et al., 2023b). While useful, they leave open the “causal parrot” concern (Zečević et al., 2023): models can succeed with memorized causal facts or linguistic cues rather than causal reasoning behaviors needed to discover causal mechanisms (Zheng et al., 2023; Liu et al., 2023).

To illustrate, let’s consider the following thought experiment. Suppose we are interested in studying the

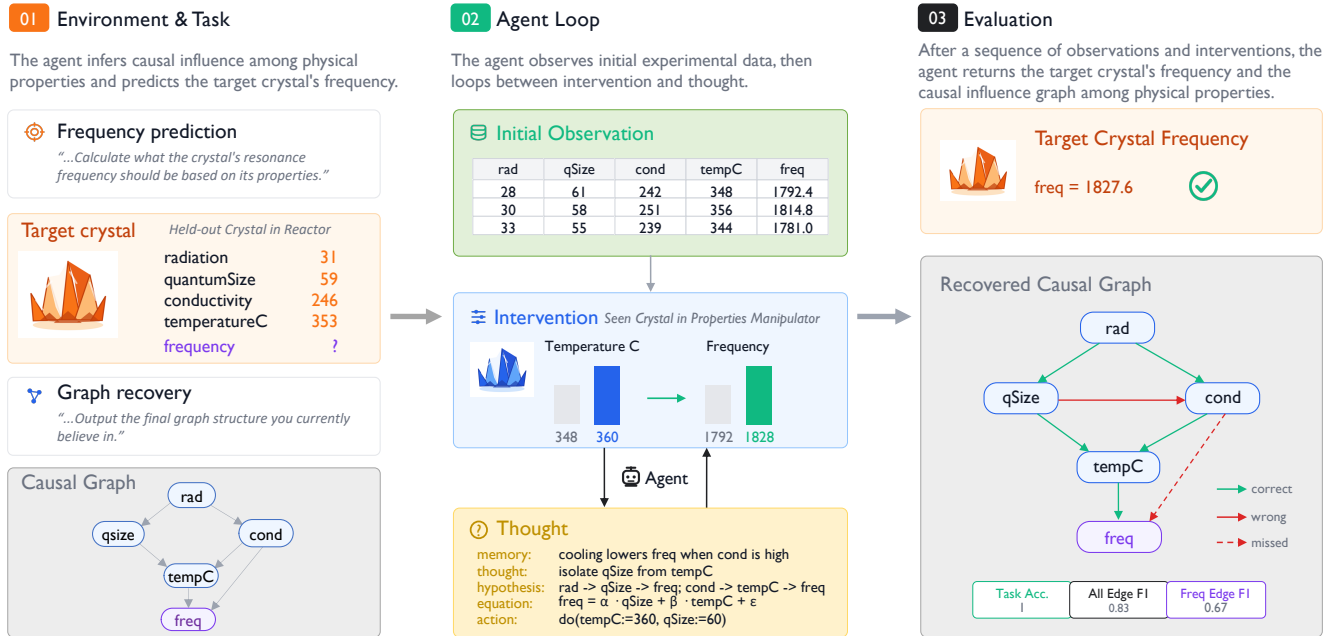


Figure 1: Overview of a *CausaLab* episode. (1) The environment instantiates a hidden SCM — a causal graph over crystal properties plus structural equations and coefficients — and uses it to generate prior measurement records, a manipulator crystal, and a held-out reactor crystal. All are governed by the same SCM but have different property values. (2) The agent observes measured properties and frequency values in the prior records, then chooses, within a budget, interventions on the manipulator crystal through the property manipulator. (3) At every step the agent emits a DSL hypothesis (graph, structural equation for frequency, coefficients) that we parse against the ground-truth SCM. (4) The agent predicts the held-out frequency of the reactor crystal; we score the final prediction *and* the trajectory of recovered mechanisms.

causal relationship between temperature and the resonance frequency of a crystal. An LLM agent might appear useful in at least two different ways. (1) It may retrieve from existing sources, such as Wikipedia or its training data, that temperature causes resonance frequency. (2) It may observe paired measurements of temperature and frequency, formulate hypotheses, design experiments, perform interventions, observe the resulting changes, and infer causation from evidence (Pearl, 2009; Hauser and Bühlmann, 2012; Lampinen et al., 2023). While both are valuable in practice, (1) offers little help when the relevant causal knowledge lies beyond the current frontier of human knowledge. We therefore argue that (2) is especially important, particularly for important applications such as scientific discovery, because it enables LLM agents to help advance the frontiers of knowledge in a manner closer to what human scientists would do (Langley, 2019; Dunbar and Fugelsang, 2005; Jansen et al., 2024).

We introduce *CausaLab* (Figure 1), a scalable environment for evaluating LLM agents as interactive causal discoverers, joining a recent line of interactive scientific-agent and causal-discovery benchmarks (Jansen et al., 2024; Havrilla et al., 2025; Chen et al., 2026, 2025; Geng et al., 2025). Each episode is generated by a hidden structural causal model (SCM) (Pearl, 2009): a causal graph together with structural equations that determine crystal properties and frequency. The agent receives prior measurement records, can run budgeted interventions on a manipulator crystal through a property manipulator, and must predict the frequency of a separate reactor crystal governed by the same SCM (Figure 1; §3). Two design choices distinguish *CausaLab* from prior causal-reasoning evaluations. First, the hidden SCM is sampled per episode rather than

drawn from public causal corpora, which sidesteps the “causal parrot” concern that scores reflect memorized causal lexicon. Second, a lightweight domain-specific language (DSL; §4) records the agent’s accumulated evidence, current graph and equation hypothesis, planned experiment, and action at each step, so we can score not only the final prediction but also the trajectory-level faithfulness of the recovered mechanism to the ground-truth SCM (§5).

Our experiments span closed and open-weight models, multiple model sizes, and thinking versus non-thinking variants, surfacing four findings that prior static benchmarks cannot reach. **(1) Correct predictions often do not reflect correct mechanism discovery.** Across matched functional-form, hidden-perturbation, and target-edge controls, endpoint accuracy and mechanism fidelity move separately: agents can find plausible parents while missing quantitative equations, preserve task success while degrading all-edge recovery, or lose accuracy mainly when the target equation itself is perturbed. **(2) Observation-conditioned online intervention best balances prediction and graph recovery.** Pure observation can boost endpoint accuracy without recovering structure, and pure intervention is weak before observations narrow the hypothesis space. For GPT-5.2-high on 6-node graphs, pure observation reaches 92% accuracy but only 0.47 all-edge F_1 , while mixed online observation-intervention reaches 80%/0.80. Offline intervention traces do not replace online experimental choice: injecting “Golden” chains raises GPT-5-mini accuracy to 90% on 4 nodes while lowering all-edge F_1 . **(3) Model family and scale pay off unevenly across the two axes.** GPT-5.2-high has the best endpoint accuracy and lowest directed all-edge SHD at every graph size, but gains are not uniform across graph sizes or metrics. Open-weight Qwen3.5 can approach GPT-5-mini on some task scores, yet its SHD rises faster as graphs grow; thinking generally lowers Qwen SHD. Even GPT-5.2-high drops to 64% accuracy and directed SHD 4.761 at 7 nodes. **(4) Many failures come from premature commitment, not exhausted budget.** Both successful and failed runs leave roughly half the intervention budget unspent, failed runs end with hypotheses inconsistent with their own data, and a single explicit verification step lifts 4-node accuracy from 48% to 60%. *CausaLab* therefore separates predictive success from causal understanding, revealing how current LLM agents still struggle to explore unfamiliar environments interactively, test candidate mechanisms, and revise toward the causal regularities that govern them.

2. Background and Related Work

Causal reasoning goes beyond associational prediction by asking how a system would change under interventions and counterfactual alternatives (Pearl, 2009; Pearl and Mackenzie, 2018; Imbens and Rubin, 2015). Structural causal models (SCMs) formalize these assumptions as directed graphs plus structural equations (Pearl, 2009). In *CausaLab*, each episode’s hidden SCM is both the ground truth (§3.1) and the evaluation target (§3.3), letting us score whether an agent recovers the graph and target equation, not only whether it predicts the reactor value.

Most LLM causal evaluations are static: they ask models to answer textual causal questions, reason over given graphs, classify cause-effect direction, or solve formal causal-inference queries (Kiciman et al., 2023; Jin et al., 2023a,b; Chen et al., 2024b; Wang, 2024; Chen et al., 2024a). Related work also uses LLMs as causal priors for edge scoring, causal ordering, or query-efficient discovery (Long et al., 2023; Darvari et al., 2024; Vashishtha et al., 2023; Jiralerspong et al., 2024). Recent SCM-oriented studies either use LLM metadata reasoning to support graph discovery (Abdulaal et al., 2024) or test coefficient elicitation when the DAG is supplied (Yamaoka et al., 2026). These settings clarify what causal knowledge LLMs can express, but they usually provide the variables, evidence, graph, or query up front. *CausaLab* instead asks whether an LLM agent can gather evidence, revise a hypothesis, and transfer the learned mechanism to a new instance, all within a scientific-discovery setting that offers no hints about the underlying causal structure.

Interactive environments broaden evaluation beyond one-shot answers, including scientific-discovery worlds, budgeted graph-discovery games, causal games, and non-LLM intervention planners (Jansen et al., 2024; Havrilla et al., 2025; Chen et al., 2026; Gregorini et al., 2025). A basic agent scaffold for such settings is ReAct-style reasoning and acting, where the model interleaves deliberation with executable environment actions (Yao et al., 2023). The closest recent benchmark is Auto-Bench, where LLM agents iteratively query scientific or social-network environments to recover a hidden causal graph (Chen et al., 2025). Work on black-box reverse engineering similarly shows that actively designing queries is not equivalent to receiving another agent’s intervention data (Geng et al., 2025).

CausaLab differs from Auto-Bench in its evaluation target. Auto-Bench primarily asks whether an agent can discover a hidden DAG through interaction. *CausaLab* asks whether the discovered mechanism *transfers*: after learning from prior measurements and interventions on a manipulator crystal, the agent must predict a held-out reactor crystal generated by the same SCM, while its per-step DSL hypotheses expose the graph, the frequency structural equation, and the coefficients it is committing to. This makes it possible to separate task utility from structural and quantitative faithfulness, and to audit how an LLM agent revises or fails to revise an explicit SCM over time.

This connects two evaluation traditions: explicit SCM recovery from causal discovery and sequential experiment design from agent benchmarks. Because each episode has a known ground-truth SCM and a logged interaction trace, *CausaLab* can score both final-task utility and the faithfulness of the recovered mechanism.

3. The Construction of CausaLab

This section first defines the episode-level task and what the agent must infer, then specifies the SCM in §3.1, the observation and intervention protocol in §3.2, and the evaluation targets in §3.3. Artifact, licensing, and implementation details are provided in Appendix A.3.

Design principles. The benchmark is designed around three goals. First, can a model infer a causal mechanism that transfers to a new instance, rather than fitting an isolated value pattern? Second, can it choose informative interventions rather than passively consume a fixed dataset? Third, how do these abilities scale with graph size, topology, functional form, intervention budget, and hidden disturbances? The corresponding design choices that realize these goals are shared-mechanism transfer between two crystals, online intervention choice, and synthetically controlled SCM generation with known ground truth.

Task formulation. A *CausaLab* episode is a transfer problem under a hidden SCM: the causal graph, structural equations, and coefficients are all hidden, and the agent is given only prior measurement records plus a finite budget for interventions (Figure 1). The episode also contains two crystals generated by the same SCM: a manipulator crystal on which the agent may intervene, and a reactor crystal whose frequency is held out. The initial records contain physical properties and resulting frequency values from earlier measurements under the same SCM. The agent then spends its interaction budget on interventions over controllable non-frequency properties of the manipulator crystal and observes the resulting measurements. After collecting this evidence, the agent predicts the hidden frequency of the reactor crystal. The records, manipulator crystal, and reactor crystal share the same SCM but have different property values, so the agent cannot solve the task by copying an observed frequency; it must infer a mechanism that transfers.

The agent is told the property names and functional family but receives interventions only on a configured subset $C \subseteq O$ of controllable observable non-frequency variables; variables outside C (including Y and any non-controllable property) are observable but not intervenable. The reactor crystal exposes only its non-frequency variables; per-variable access is summarized in Appendix Table 2. At each step the agent also emits a DSL hypothesis that we parse into a directed graph, frequency equation, and coefficients. Solving an episode therefore requires both a correct reactor prediction and a causal hypothesis that matches the hidden SCM under the metrics of §3.3.

3.1. Structural Causal Models

Each episode instantiates an SCM $\mathcal{M} = (\mathbf{U}, \mathbf{V}, F, P(\mathbf{U}))$ (Pearl, 2009). Here \mathbf{U} are exogenous source terms, \mathbf{V} are endogenous variables, F is the set of structural equations, and $P(\mathbf{U})$ is the exogenous distribution. In *CausaLab*, the endogenous variables are observable properties O plus the target $Y = \text{frequency}$. Root variables are endogenous nodes whose values are generated from exogenous source terms, and optional hidden-noise terms are also exogenous. We sample a DAG G over $\mathbf{V} = O \cup \{Y\}$, assign root nodes from their exogenous sources, then compute non-root variables in topological order. In the linear family,

$$X = b + \sum_{p \in \text{pa}(X)} w_p p,$$

and in the quadratic family,

$$X = b + \sum_{p \in \text{pa}(X)} (u_p p^2 + w_p p).$$

The sampled graph, equations, and coefficients, including the base value of frequency, are shared across the prior records, manipulator crystal, and reactor crystal; controllable-property base values differ across these instances. This asymmetry is what forces the agent to infer how variables are connected and then apply that mechanism to the reactor’s property values.

Some graph families also include an unobserved exogenous disturbance H that perturbs the system as follows. After every intervention, H is resampled and added as a fixed-weight shift to a designated subset of observable endogenous variables; those shifted values then propagate downstream through F . H itself is not in \mathbf{V} , is not named to the agent, and cannot be observed or set directly — the agent sees only its downstream effects on the returned variable values. These settings test whether an agent can distinguish a stable causal mechanism from post-intervention noise. Additional distributions and coefficient ranges appear in Appendix A; formal SCM and hidden-disturbance details appear in Appendix A.2.

3.2. Interaction and Outputs

Each episode proceeds through a repeated hypothesis–experiment loop. The agent receives an initial batch of measurement records, including non-frequency properties and the resulting frequency. It may then intervene by setting one controllable non-frequency property on the manipulator crystal; the environment recomputes that crystal’s resulting measurement under the hidden SCM and returns it to the agent. The reactor crystal is observed but not intervened on: its non-frequency properties are visible, and its frequency remains hidden until the agent submits a final value.

Concretely, the loop begins with the initial observation batch and then alternates between interventions and observations: *choose an intervention on one controllable manipulator-crystal property* → *observe the resulting manipulator-crystal measurement* → *revise the DSL hypothesis and choose the next intervention*.

For example, after seeing several prior measurement records, an agent may set the manipulator crystal’s radiation to a chosen value, see how temperature, conductivity, and frequency change, and then decide whether the evidence supports a direct edge into frequency or an indirect path through another property. This is the interaction that Figure 1 depicts at the task level and Appendix Figure 8 exposes at the trajectory level.

The intervention semantics are shift-style rather than hard $\text{do}(X=v)$ (Rothenhäusler et al., 2015), and we specify them here because they determine what the agent’s returned observations mean. For a controllable variable $X \in C$, an intervention request with value v replaces the base term in that variable’s structural equation for the next environment update:

$$X \leftarrow v + \sum_{p \in \text{pa}(X)} w_p p$$

in the linear family, and analogously

$$X \leftarrow v + \sum_{p \in \text{pa}(X)} (u_p p^2 + w_p p)$$

in the quadratic family. Incoming parent contributions are therefore retained; only the intercept/base component is shifted. A hard intervention would instead force $X = v$ and sever incoming causal influence.

At the end of the episode, the agent submits a numeric prediction for the reactor frequency and a final DSL hypothesis specifying causal edges, the proposed structural equation for frequency, and coefficients. The same DSL can be emitted at intermediate steps, giving a trajectory of evolving hypotheses.

3.3. Evaluation

We evaluate whether the model both solves the held-out task and recovers the mechanism needed to solve it causally. Task success is frequency accuracy on the reactor crystal. Mechanism recovery compares the parsed DSL hypothesis against the ground-truth SCM: graph precision, recall, and F_1 measure recovered causal edges; structural Hamming distance (SHD) counts missing, extra, and reversed directed edges, with lower values indicating closer graph recovery; coefficient F_1 measures whether the quantitative frequency mechanism is correct; and root-node identification measures whether the agent distinguishes exogenous/-root variables from mediated variables. This separation is essential: an agent may predict the held-out frequency without recovering the SCM, or recover the qualitative graph while missing the coefficients needed for reliable transfer. A correct solution therefore requires three linked behaviors: collect useful observational/interventional evidence, infer a graph and target equation that explain the prior records and manipulator-crystal measurements, and apply that mechanism to the reactor crystal’s observed properties.

4. A DSL for Causal Trajectories

At each interaction step t , the agent emits a compact DSL record with five fields: *Memory* M_t , the persistent episode notes; *Thought* T_t , a short interpretation of the current evidence; *Past data* $\mathcal{D}_{\leq t}$, the accumulated observations and intervention outcomes; *Hypothesis* H_t , the current causal claim; and *Experiment* E_t , the next planned intervention and its rationale. Only H_t is used as a scored causal artifact: it states hypothesized edges, the structural equation for frequency, and the associated coefficients. Appendix Figure 8 shows how parsed hypotheses are rendered as candidate graphs and recovery metrics over time. Prompting and repair details appear in Appendix A.5.

Making the hypothesis parsable. We make H_t a scored object by requiring a fixed schema rather than free-form prose. The schema contains three typed parts: directed edges as (parent, child) pairs over episode variables, a frequency structural equation in the declared functional family, and numeric coefficients for the equation terms. A deterministic parser converts each valid hypothesis into a candidate graph G_t and target mechanism \hat{f}_t , producing a trajectory $\{(G_t, \hat{f}_t)\}_{t=1}^T$. This lets the benchmark score the mechanism the agent commits to at each step using the same graph, root, and coefficient metrics used for final evaluation, rather than relying only on the final numeric answer.

5. Experiments

We use *CausaLab* to ask four questions. (RQ1) Does correct prediction imply mechanism recovery? (RQ2) Which interaction regime best balances task accuracy and graph recovery, and can offline intervention traces replace online experimental choice? (RQ3) How do model family, scale, and thinking traces affect prediction and mechanism recovery across graph sizes? (RQ4) Why do agents fail, and what simple check can reduce these failures? The paired prediction and SCM-recovery targets separate task success from mechanism faithfulness, and DSL traces expose the hypotheses agents commit to.

5.1. Experimental Setup

Setup. The main suite evaluates four models—GPT-5-mini, GPT-5.2-high, Qwen3.5-Thinking, and Qwen3.5-Non-thinking—on *CausaLab*’s 3–7 node graph families, with up to 50 topologies per (graph size, model) cell and one run per task. Observation–intervention scaling experiments use GPT-5-mini and GPT-5.2-high on the 4-node and 6-node suites. Targeted follow-ups use the 4-/6-node suites, primarily with GPT-5-mini. All runs use temperature 0.1 and fixed observation/intervention budgets per graph size (Appendix A). The reactor crystal’s hidden frequency is the target in every episode, so end-task accuracy is the exact prediction rate for that value; mechanism recovery is scored separately with graph, parent, root, edge, and coefficient metrics against the full episode SCM. Except for the explicit observation–intervention scaling suite, all follow-up analyses use the mixed regime with two initial observations; RQ2 motivates this setting as the anchor for subsequent analyses.

5.2. RQ1: Correct Frequency Prediction Does Not Imply Mechanism Recovery

CausaLab pairs each episode with a ground-truth SCM, so we can score the answer and the mechanism separately. Three controls show that these axes split in different ways rather than collapsing to one scalar.

Function form. Holding the 50 four-node topologies fixed but replacing the linear mechanism with a hard-quadratic one cuts GPT-5-mini accuracy from 48% to 24% (Figure 2). The graph is not simply lost: root-node F_1 rises (0.559→0.829) and edge precision is preserved, but frequency-weight F_1 collapses (0.589→0.251; Appendix Table 3). The agent can find plausible parents and still fail because it misses the quantitative mechanism.

Hidden perturbations. Off-target hidden noise leaves accuracy near baseline (40–54% versus 48%) but lowers all-edge F_1 from 0.79 to 0.61–0.70. When the hidden disturbance can perturb frequency itself, accuracy drops to 26–40% (Appendix Figure 9; Appendix Table 4), showing that some successful predictions

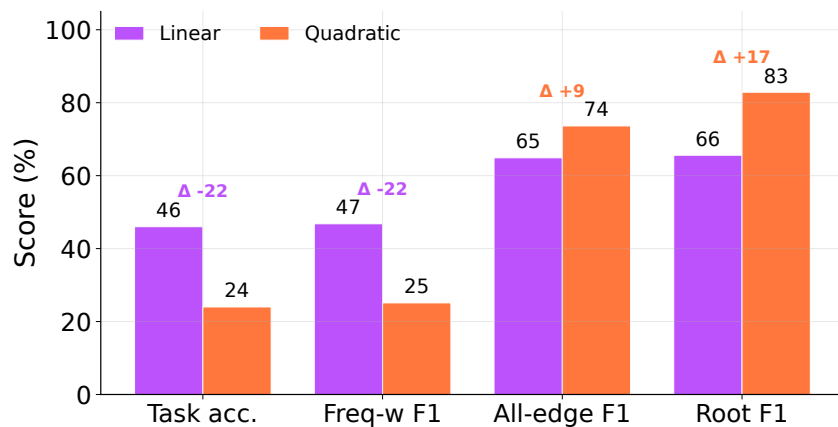


Figure 2: Matched 4-node comparison between linear and hard-quadratic mechanisms for GPT-5-mini. Topology is fixed; only the functional form changes. Task accuracy and frequency-weight F_1 collapse while all-edge and root-node F_1 are preserved or even rise — agents lose the mechanism, not the graph.

came from fitting a local target equation rather than recovering a mechanism robust to hidden target perturbations.

Target outgoing edges. FreqParent keeps mean edge counts matched but lets frequency have outgoing edges. Accuracy rises on 4- and 6-node graphs because the target has fewer incoming edges to fit, while all-edge recovery falls because global directionality is harder (Appendix Figure 10; Appendix Table 5).

Takeaway

Prediction accuracy is necessary but not sufficient evidence of mechanism recovery.

5.3. RQ2: Observation-Conditioned Online Intervention Outperforms Pure and Offline Regimes

RQ2 separates two questions: whether agents need observations, interventions, or both; and whether offline intervention data is enough when the agent does not choose the experiments online. Figure 3 summarizes the three online regimes across our four scaling families. For GPT-5-mini, pure observation often gives the strongest end-task accuracy on the easier graphs, but mixed observation-conditioned intervention consistently recovers more faithful graphs on both the 4-node and 6-node families. In the GPT-5.2-high 6-node setting, for example, observation-only has higher accuracy than mixed (92% versus 80%) but much lower graph-recovery F_1 (0.47 versus 0.80). Pure intervention is weak on both axes, becoming useful only after observation narrows the hypothesis space. We therefore use mixed online regimes as the anchor for follow-up controls. The full regime scatter appears in Appendix Figure 12; full scaling curves and tables appear in Appendix Figures 13 and 14 and Appendix A.9.

The *Golden* control then separates offline intervention data from online intervention decisions by giving the agent a bounded low-MEC intervention chain instead of letting it intervene online. Golden improves task accuracy above the main suite baselines (90% versus 48% on 4-node graphs, 44% versus 24% on 6-node graphs) but drops all-edge F_1 on both sizes (Figure 4; Appendix Table 6). High-quality intervention chains therefore behave mostly like stronger observations: they help fit the target equation, but they do not replace the structural signal supplied by the agent’s own online intervention loop.

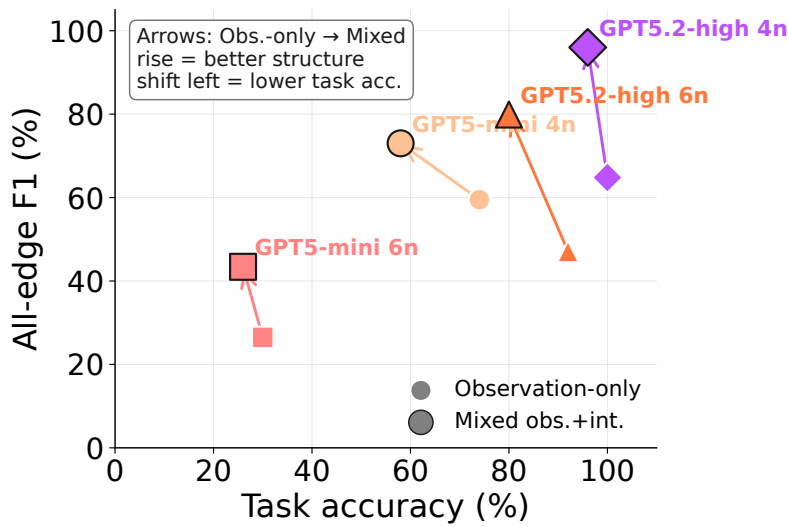


Figure 3: Prediction-versus-recovery gap across the four scaling families. Each suite is shown as an Obs.-only → Mixed arrow in (task accuracy, all-edge F_1) space: mixed regimes consistently shift mass toward higher graph fidelity at comparable or better task accuracy.

Takeaway

Observation-conditioned online intervention gives the best balance: observations narrow the hypothesis space, while agent-chosen interventions recover more faithful graphs.

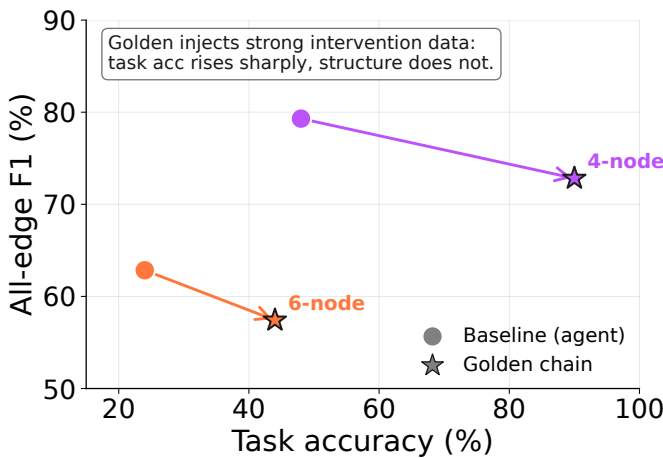


Figure 4: Golden-intervention experiments on GPT-5-mini. Baseline → Golden arrows in (task accuracy, all-edge F_1) space: injected low-MEC intervention traces improve frequency prediction but hurt all-edge recovery, separating intervention data from intervention choice.

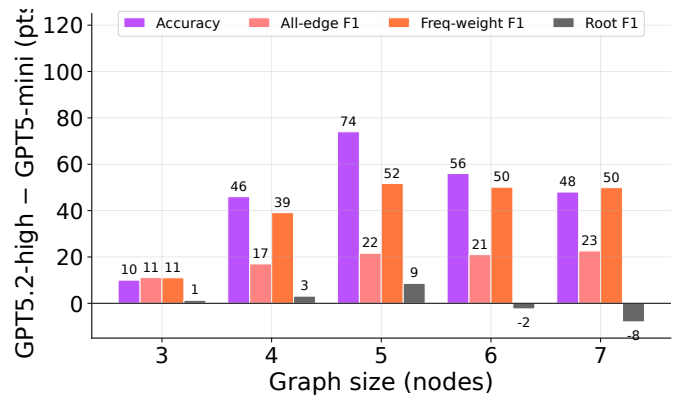


Figure 5: Capability gap (GPT-5.2-high - GPT-5-mini) in percentage points across graph sizes and metrics. Scaling concentrates in accuracy and frequency-weight F_1 ; root-node gains are near zero or negative at 6-7 nodes, showing where larger models still stall.

5.4. RQ3: Model Family and Scale Pay Off Unevenly Across the Two Axes

GPT-5.2-high outperforms GPT-5-mini across graph sizes, but the gains concentrate on mediated structure and quantitative mechanism fitting rather than every metric uniformly. Figure 6 extends the model-family comparison to all 3–7 node main suites, covering the two GPT models and Qwen3.5 with and without thinking traces. GPT-5.2-high is the strongest model overall, with the best endpoint accuracy and lowest directed all-edge SHD at every graph size. Open-weight Qwen3.5 models can be competitive with GPT-5-mini on some task scores, but their SHD rises faster as graph size grows. Thinking generally improves Qwen structure recovery, lowering SHD at four graph sizes and raising all-edge F_1 at every measured size. Across the full 3–7 node sweep, even GPT-5.2-high still drops to 64% accuracy and directed SHD 4.761 at 7 nodes (Figure 6), and the per-metric gap (Figure 5) concentrates in accuracy and frequency-weight F_1 while root-node gains flatten on 6–7 node graphs. Absolute metric trajectories appear in Appendix Figure 11; per-model metrics are in Appendix A.9.

Takeaway

Scaling improves direct-parent and coefficient recovery, but does not remove the need for better exploration and mechanism-checking methods; thinking helps Qwen recover structure over most graph sizes, but does not close the gap to the strongest GPT model.

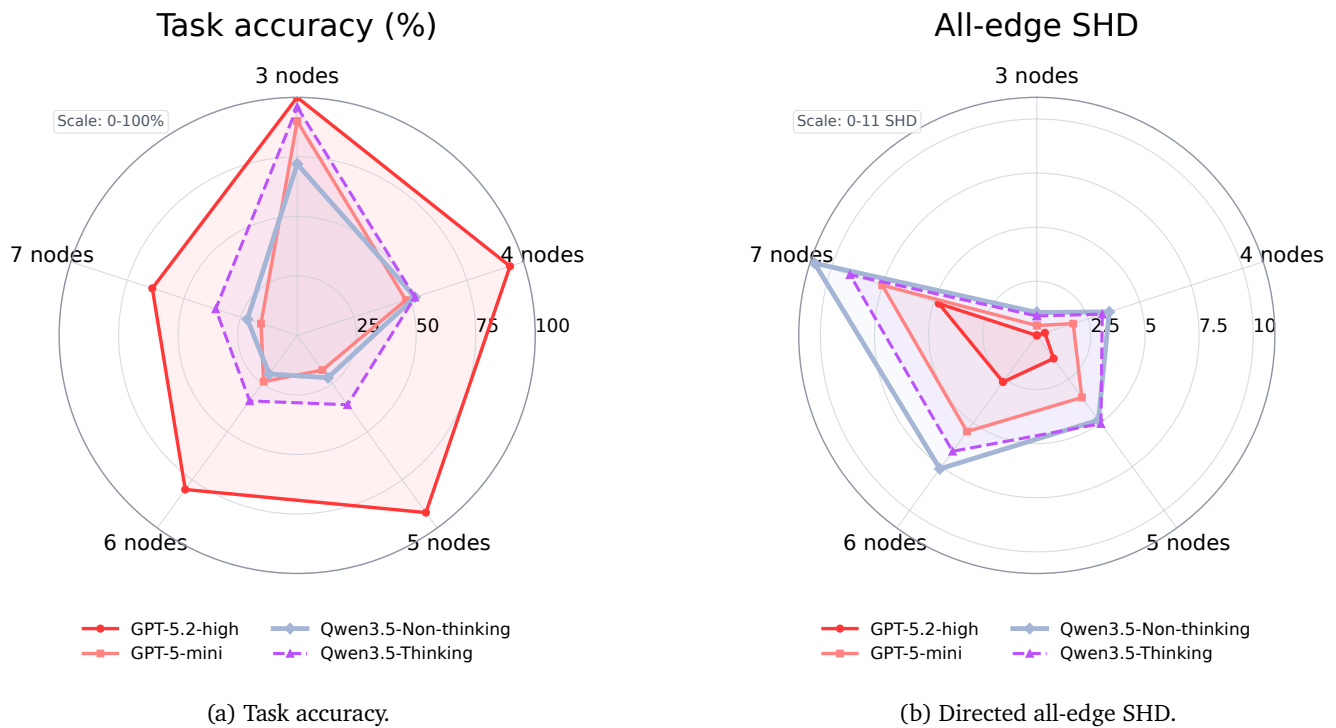


Figure 6: Four-model comparison across the 3–7 node main suites. Each vertex fixes graph size and compares GPT-5.2-high, GPT-5-mini, Qwen3.5-Thinking, and Qwen3.5-Non-thinking. Lower SHD is better; a reversed edge counts as one directed SHD error. Task values are endpoint reactor accuracies.

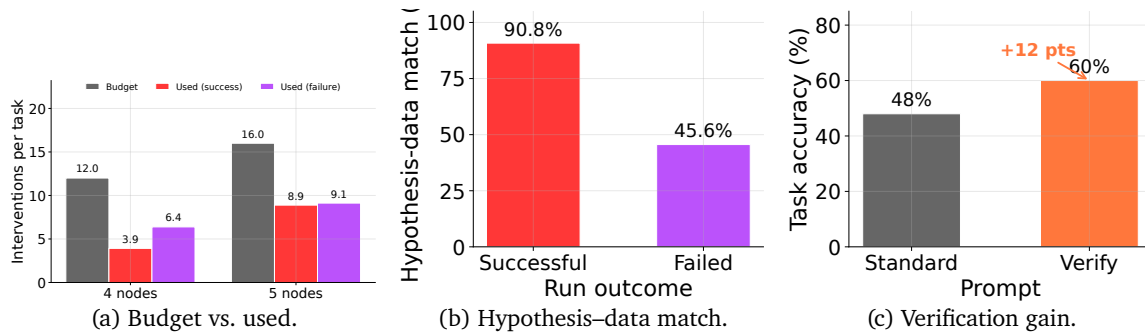


Figure 7: Early-commitment diagnostics for GPT-5-mini: both outcome groups leave roughly half the budget unused; failed hypotheses fit collected data worse; one verification step raises 4-node accuracy from 48% to 60%.

5.5. RQ4: Agents Fail by Stopping Early, and a Single Verification Step Helps

The DSL trajectories show that failure is often early commitment rather than missing data. Across the main 4-node and 5-node experiments, both successful and failed runs leave about half of the intervention budget unused, and simply granting more budget yields only modest accuracy gains (Figure 7, left). The DSL lets us inspect *why* agents stop: at the step where each run commits to a final answer, we compare the recorded hypothesis H_t (graph + structural equation + coefficients) against the data already collected. Successful runs mostly end with hypotheses consistent with their own $\mathcal{D}_{\leq t}$, while failed runs end with hypotheses that mispredict the very observations and intervention outcomes that produced them. The “hypothesis–data match” axis reports the mean percentage of collected data points whose recorded frequency is reproduced by the final hypothesis equation within numerical tolerance. The failure mode is therefore better described as *overconfidence*: agents treat an unverified hypothesis as a final theory rather than continuing to spend budget on disambiguating experiments. Consistent with this reading, a single explicit verification step that checks H_T against $\mathcal{D}_{\leq T}$ before committing raises 4-node accuracy from 48% to 60% (Figure 7, right), making verification a cheap model-agnostic fix for a failure mode that only appears when the benchmark records the trajectory.

Takeaway

Many failures are not caused by an exhausted budget; they are caused by committing before checking whether the proposed SCM explains the evidence already collected.

6. Discussion and Conclusion

CausaLab should be read as a controlled stress test for interactive causal discovery, not as a broad claim about causal reasoning in arbitrary real-world systems. Its scope is synthetic 3–7 node SCMs, mostly linear mechanisms with one quadratic family, a limited set of model families, and shift-style interventions that adjust variables through the laboratory interface rather than implement perfect hard-*do* operations. Within that scope, the benchmark shows that agents can collect useful evidence and predict the held-out frequency while still recovering an incomplete or wrong mechanism. By scoring both final prediction and the evolving SCM hypothesis, *CausaLab* exposes where scale helps and where graph complexity, quantitative mechanism fitting, and premature hypothesis commitment remain central bottlenecks.

7. Potential Risks

CausaLab is a synthetic benchmark, so its results should not be read as evidence that an agent is ready for real scientific, medical, or policy deployment. The main risk is overgeneralizing success on templated SCM tasks to high-stakes settings with real interventions and domain constraints.

8. Limitations

CausaLab is a controlled synthetic benchmark, so its results should be interpreted within that scope. The current suites use 3–7 node SCMs with mostly linear mechanisms and one hard-quadratic extension, so they do not cover the full range of causal structures, functional forms, latent variables, or measurement processes found in real scientific domains.

Our experiments cover a finite set of LLM agents, prompts, and interaction budgets. Performance may differ with other models, tool interfaces, decoding policies, or longer exploration budgets, and our main analyses focus on final predictions and final hypotheses rather than every possible trajectory-level diagnostic.

References

- Ahmed Abdulaal, adamos hadjivasiliou, Nina Montana-Brown, Tiantian He, Ayodeji Ijishakin, Ivana Drobnjak, Daniel C. Castro, and Daniel C. Alexander. Causal modelling agents: Causal graph discovery through synergising metadata- and data-driven reasoning. In *The Twelfth International Conference on Learning Representations*, 2024. URL <https://openreview.net/forum?id=pAoqRlTBtY>.
- Steen A. Andersson, David Madigan, and Michael D. Perlman. A characterization of Markov equivalence classes for acyclic digraphs. *The Annals of Statistics*, 25(2):505 – 541, 1997. doi: 10.1214/aos/1031833662. URL <https://doi.org/10.1214/aos/1031833662>.
- Sirui Chen, Bo Peng, Meiqi Chen, Ruiqi Wang, Mengying Xu, Xingyu Zeng, Rui Zhao, Shengjie Zhao, Yu Qiao, and Chaochao Lu. Causal evaluation of language models, 2024a.
- Sirui Chen, Mengying Xu, Kun Wang, Xingyu Zeng, Rui Zhao, Shengjie Zhao, and Chaochao Lu. Clear: Can language models really understand causal graphs?, 2024b. URL <https://arxiv.org/abs/2406.16605>.
- Tingting Chen, Srinivas Anumasa, Beibei Lin, Vedant Shah, Anirudh Goyal, and Dianbo Liu. Auto-Bench: An automated benchmark for scientific discovery in LLMs, 2025. URL <https://arxiv.org/abs/2502.15224>.
- Zhenhao Chen, Yongqiang Chen, Chenxi Liu, Junchi Yu, Xiangchen Song, Zijian Li, Jialin Li, Philip Torr, Bo Han, and Kun Zhang. Causalgame: Benchmarking causal thinking of llm agents in games. In *ICLR 2026 Workshop on Foundation Models for Science*, 2026. URL <https://openreview.net/forum?id=SEFSkn416d>.
- Victor-Alexandru Darvariou, Stephen Hailes, and Mirco Musolesi. Large language models are effective priors for causal graph discovery, 2024. URL <https://arxiv.org/abs/2405.13551>.
- K. Dunbar and J. Fugelsang. Causal thinking in science: How scientists and students interpret the unexpected. In M. E. Gorman, R. D. Tweney, D. C. Gooding, and A. P. Kincannon, editors, *Scientific and Technological Thinking*, pages 57–79. Lawrence Erlbaum Associates, Mahwah, NJ, 2005.
- Jiayi Geng, Howard Chen, Dilip Arumugam, and Thomas L. Griffiths. Are large language models reliable AI scientists? assessing reverse-engineering of black-box systems, 2025. URL <https://arxiv.org/abs/2505.17968>.
- Matteo Gregorini, Chiara Boldrini, and Lorenzo Valerio. DODO: Causal structure learning with budgeted interventions, 2025. URL <https://arxiv.org/abs/2510.08207>.

- Alain Hauser and Peter Bühlmann. Characterization and greedy learning of interventional markov equivalence classes of directed acyclic graphs. *Journal of Machine Learning Research*, 13(79):2409–2464, 2012. URL <http://jmlr.org/papers/v13/hauser12a.html>.
- Alex Havrilla, David Alvarez-Melis, and Nicolo Fusi. Igda: Interactive graph discovery through large language model agents, 2025. URL <https://arxiv.org/abs/2502.17189>.
- Guido W. Imbens and Donald B. Rubin. *Causal Inference for Statistics, Social, and Biomedical Sciences*. Cambridge University Press, 2015. ISBN 978-0521885884. doi: 10.1017/CBO9781139025751. URL <https://doi.org/10.1017/CBO9781139025751>.
- Peter A. Jansen, Marc-Alexandre Côté, Tushar Khot, Erin Bransom, Bhavana Dalvi Mishra, Bodhisattwa Prasad Majumder, Oyvind Tafjord, and Peter Clark. DISCOVERYWORLD: A virtual environment for developing and evaluating automated scientific discovery agents. *CoRR*, abs/2406.06769, 2024. doi: 10.48550/ARXIV.2406.06769. URL <https://doi.org/10.48550/arXiv.2406.06769>.
- Liwei Jiang, Taylor Sorensen, Sydney Levine, and Yejin Choi. Can language models reason about individualistic human values and preferences? *arXiv:2410.03868*, 2024.
- Zhijing Jin, Yuen Chen, Felix Leeb, Luigi Gresele, Ojasv Kamal, Zhiheng LYU, Kevin Blin, Fernando Gonzalez Adatao, Max Kleiman-Weiner, Mrinmaya Sachan, and Bernhard Schölkopf. Cladder: Assessing causal reasoning in language models. In A. Oh, T. Naumann, A. Globerson, K. Saenko, M. Hardt, and S. Levine, editors, *Proceedings of the Advances in Neural Information Processing Systems*, 2023a. doi: 10.48550/ARXIV.2312.04350. URL <https://doi.org/10.48550/arXiv.2312.04350>.
- Zhijing Jin, Jiarui Liu, Zhiheng Lyu, Spencer Poff, Mrinmaya Sachan, Rada Mihalcea, Mona Diab, and Bernhard Schölkopf. Can large language models infer causation from correlation?, 2023b. URL <https://arxiv.org/abs/2306.05836>.
- Thomas Jiralerspong, Xiaoyin Chen, Yash More, Vedant Shah, and Yoshua Bengio. Efficient causal graph discovery using large language models, 2024. URL <https://arxiv.org/abs/2402.01207>.
- Emre Kıcıman, Robert Ness, Amit Sharma, and Chenhao Tan. Causal reasoning and large language models: Opening a new frontier for causality, 2023. URL <https://arxiv.org/abs/2305.00050>.
- Andrew K. Lampinen, Stephanie C. Y. Chan, Ishita Dasgupta, Andrew J. Nam, and Jane X. Wang. Passive learning of active causal strategies in agents and language models. In *Proceedings of the Advances in Neural Information Processing Systems*, 2023.
- Pat Langley. Scientific discovery, causal explanation, and process model induction. *Mind & Society*, 18(1):43–56, 2019. doi: 10.1007/s11299-019-00216-1. URL <https://doi.org/10.1007/s11299-019-00216-1>.
- Jintao Liu, Zequn Zhang, Zhi Guo, Li Jin, Xiaoyu Li, Kaiwen Wei, and Xian Sun. Kept: Knowledge enhanced prompt tuning for event causality identification. *KnowledgeBased Systems*, 259, 2023.
- Stephanie Long, Tibor Schuster, and Alexandre Piché. Can large language models build causal graphs?, 2023. URL <https://arxiv.org/abs/2303.05279>.
- Joris M. Mooij, Sara Magliacane, and Tom Claassen. Joint causal inference from multiple contexts. *Journal of Machine Learning Research*, 21(99):1–108, 2020. URL <http://jmlr.org/papers/v21/17-123.html>.
- Judea Pearl. *Causality: Models, Reasoning, and Inference*. Cambridge University Press, 2 edition, sep 2009. ISBN 9780511803161. doi: 10.1017/cbo9780511803161. URL <https://doi.org/10.1017/CBO9780511803161>.
- Judea Pearl and Dana Mackenzie. *The Book of Why: The New Science of Cause and Effect*. Basic Books, Inc., USA, 1st edition, 2018. ISBN 046509760X.

- Lianhui Qin, Antoine Bosselut, Ari Holtzman, Chandra Bhagavatula, Elizabeth Clark, and Yejin Choi. Counterfactual story reasoning and generation. In *Proceedings of the 2019 Conference on Empirical Methods in Natural Language Processing and the 9th International Joint Conference on Natural Language Processing (EMNLP-IJCNLP)*, pages 5043–5053, Hong Kong, China, November 2019. Association for Computational Linguistics. doi: 10.18653/v1/D19-1509. URL <https://aclanthology.org/D19-1509/>.
- Angelika Romanou, Syrielle Montariol, Debjit Paul, Léo Laugier, Karl Aberer, and Antoine Bosselut. Crab: Assessing the strength of causal relationships between real-world events. In *Proceedings of the 2023 Conference on Empirical Methods in Natural Language Processing (EMNLP 2023)*, pages 15198–15216, 2023. doi: 10.18653/V1/2023.EMNLP-MAIN.940. URL <https://aclanthology.org/2023.emnlp-main.940.pdf>.
- Dominik Rothenhäusler, Christina Heinze, Jonas Peters, and Nicolai Meinshausen. backshift: Learning causal cyclic graphs from unknown shift interventions, 2015. URL <https://arxiv.org/abs/1506.02494>.
- Alessandro Stolfo, Zhijing Jin, Kumar Shridhar, Bernhard Schölkopf, and Mrinmaya Sachan. A causal framework to quantify the robustness of mathematical reasoning with language models. In *Proceedings of the 61st Annual Meeting of the Association for Computational Linguistics*. Association for Computational Linguistics, 2023. URL <https://arxiv.org/abs/2210.12023>.
- Aniket Vashishtha, Abbavaram Gowtham Reddy, Abhinav Kumar, Saketh Bachu, Vineeth N Balasubramanian, and Amit Sharma. Causal order: The key to leveraging imperfect experts in causal inference, 2023. URL <https://arxiv.org/abs/2310.15117>.
- Aniket Vashishtha, Abhinav Kumar, Atharva Pandey, Abbavaram Gowtham Reddy, Kabir Ahuja, Vineeth N Balasubramanian, and Amit Sharma. Teaching transformers causal reasoning through axiomatic training. In *Proceedings of the International Conference on Machine Learning*, 2025.
- Zeyu Wang. CausalBench: A comprehensive benchmark for evaluating causal reasoning capabilities of large language models. In *Proceedings of the 10th SIGHAN Workshop on Chinese Language Processing (SIGHAN-10)*, pages 143–151, Bangkok, Thailand, August 2024. Association for Computational Linguistics. URL <https://aclanthology.org/2024.sighan-1.17/>.
- Kanta Yamaoka, Sumantrak Mukherjee, Thomas Gärtner, David Antony Selby, Stefan Konigorski, Eyke Hüllermeier, Viktor Bengs, and Sebastian Josef Vollmer. Linear-LLM-SCM: Benchmarking LLMs for coefficient elicitation in linear-gaussian causal models, 2026. URL <https://arxiv.org/abs/2602.10282>.
- Shunyu Yao, Jeffrey Zhao, Dian Yu, Nan Du, Izhak Shafran, Karthik R. Narasimhan, and Yuan Cao. React: Synergizing reasoning and acting in language models. In *The Eleventh International Conference on Learning Representations, ICLR 2023, Kigali, Rwanda, May 1-5, 2023*. OpenReview.net, 2023. URL https://openreview.net/forum?id=WE_vluYUL-X.
- Chuanqi Zang, Hanqing Wang, Mingtao Pei, and Wei Liang. Discovering the real association: Multimodal causal reasoning in video question answering. In *Proceedings of the IEEE/CVF Conference on Computer Vision and Pattern Recognition (CVPR)*, pages 19027–19036, Vancouver, Canada, June 2023. doi: 10.1109/CVPR52729.2023.01824. URL https://openaccess.thecvf.com/content/CVPR2023/html/Zang_Discovering_the_Real_Association_Multimodal_Causal_Reasoning_in_Video_Question_CVPR_2023_paper.html.
- Matej Zečević, Moritz Willig, Devendra Singh Dhami, and Kristian Kersting. Causal parrots: Large language models may talk causality but are not causal. *Transactions in Machine Learning Research*, 2023. doi: 10.48550/ARXIV.2308.13067. URL <https://arxiv.org/abs/2308.13067>.
- Junhao Zheng, Qianli Ma, Shengjie Qiu, Yue Wu, Peitian Ma, Junlong Liu, Huawen Feng, Xichen Shang, and Haibin Chen. Preserving commonsense knowledge from pre-trained language models via causal inference. In Anna Rogers, Jordan Boyd-Graber, and Naoaki Okazaki, editors, *Proceedings of the 61st Annual Meeting of the Association for Computational Linguistics (Volume 1: Long Papers)*, pages 9155–9173, Toronto, Canada, July 2023. Association for Computational Linguistics. doi: 10.18653/v1/2023.acl-long.509. URL <https://aclanthology.org/2023.acl-long.509/>.

Contents

A Appendix	16
A.1 Benchmark Setup and Causal-Discovery Context	16
A.2 SCM and Hidden-Disturbance Details	16
A.3 Artifact and Implementation Details	16
A.4 Prompt Templates	16
A.5 DSL Implementation Details	23
A.6 Trajectory-Level DSL Visualization	23
A.7 Mechanism Robustness and Perturbation Controls	23
A.8 Intervention-Trace Controls	23
A.9 Model Family and Graph-Size Scaling	24
A.10 Observation–Intervention Scaling	25

A. Appendix

A.1. Benchmark Setup and Causal-Discovery Context

This section collects setup details that are needed to interpret the main results but are too mechanical for the main text. The benchmark uses a fixed budget policy except in the explicit observation–intervention scaling suites: for a k -node graph, the observation budget is 2 and the intervention budget is $4(k - 1)$. The graph families span 3–7 node SCMs; Table 1 summarizes the topology distribution used in the main experiments.

Classical causal discovery studies how causal structure can be learned from observational, interventional, or shifted data, including constraint- and score-based discovery, interventional Markov equivalence, discovery across multiple contexts, and unknown shift interventions (Pearl, 2009; Andersson et al., 1997; Hauser and Bühlmann, 2012; Mooij et al., 2020; Rothenhäusler et al., 2015; Zang et al., 2023). *CausaLab* is closest to the shift-intervention regime of this literature, but it does not propose a new discovery algorithm or assume perfect *do*-interventions. Instead, it evaluates whether an LLM agent can recover the graph and equations of a hidden SCM through a finite sequence of shift-style interventions on controllable properties.

A.2. SCM and Hidden-Disturbance Details

Formally, each episode instantiates an SCM $\mathcal{M} = (\mathbf{U}, \mathbf{V}, F, P(\mathbf{U}))$ (Pearl, 2009): \mathbf{V} are endogenous variables determined inside the system, \mathbf{U} are exogenous variables drawn from $P(\mathbf{U})$, and F is a collection of structural equations mapping each variable’s parents and exogenous term to its value. In *CausaLab*, $\mathbf{V} = O \cup \{Y\}$, where O are observable property variables and $Y = \text{frequency}$. Root variables remain endogenous nodes, but their values are generated from exogenous source terms; in hidden-noise suites, the exogenous terms also include an unobserved disturbance H .

The agent observes O and Y in the prior evidence records, may observe and intervene on the configured subset $C \subseteq O$ of the manipulator crystal during interaction, and observes only O on the reactor crystal. Variables in $O \setminus C$ are observable but not controllable; Y is never controllable; and H , when present, is neither observable nor controllable. Hidden-disturbance suites resample H after each intervention and add it as a fixed-weight shift to a designated subset of observable endogenous variables; these shifted values then propagate downstream through the structural equations. The agent sees only the resulting observed values, not H itself.

A.3. Artifact and Implementation Details

CausaLab builds its embodied interface on DiscoveryWorld (Jansen et al., 2024), released under the Apache-2.0 license; its SCM generator, intervention/reactor mechanics, DSL traces, and scoring code are new synthetic research and evaluation artifacts. This use is consistent with DiscoveryWorld’s role as a virtual environment for evaluating scientific-discovery agents. The benchmark is generated from fixed templates over synthetic laboratory variables, so it contains no demographic attributes, personal identifiers, or naturally occurring offensive web text. Appendix A.2 and A.9 document artifact coverage, variable access, and evaluation/experiment settings.

A.4. Prompt Templates

The benchmark uses a two-stage prompting scheme. The first prompt governs iterative hypothesis–experiment interaction in the environment, while the second prompt frames the reactor activation objective and embeds the task-specific laboratory rules. The templates below are the exact prompt files used in the implementation, with runtime placeholders filled by the environment during evaluation.

Phase 1 Controller Prompt

You are playing a video game about making scientific discoveries. The game is in the style of a 2D top-down RPG (you are the agent in the center of the image), and as input you get both an image, as well as information from the user interface (provided in the JSON below) that describes your location, inventory, objects in front of you, the result of your last action, and the task that

Nodes	Graphs	Edge mean	Edge var.	Fork mean	Collider mean
3	50	2.56	0.25	0.68	0.72
4	50	4.54	1.01	2.18	2.22
5	50	7.26	4.23	5.54	5.26
6	50	8.82	5.15	6.72	6.22
7	50	10.26	4.95	7.84	7.00

Table 1: Main-experiment graph statistics. Forks and colliders are counted as three-node motif instances; edge variance is the population variance over the 50 graphs in each row.

Variable role	Observable	Intervenable
Controllable property ($X \in C$)	✓	✓
Non-controllable property ($X \in O \setminus C$)	✓	—
Target $Y = \text{frequency}$ (evidence records / manipulator crystal)	✓	—
Target $Y = \text{frequency}$ (reactor crystal)	—	—
Hidden disturbance H (when present)	—	—

Table 2: Per-variable access for the agent in a *CausaLab* episode. The agent observes prior evidence records, intervenes only on the configured controllable subset C of the manipulator crystal, and predicts the held-out frequency of the reactor crystal.

```

you're assigned to complete.
Because this is a game, the actions that you can complete are limited to a set of actions that are
defined by the game. Those are also described below.
This game is played step-by-step. At each step, you get the input that I am providing, and output a
single action to take as the next step.

Navigation note:
Moving forward moves you in the direction you're facing. You are currently facing "{{
facing_direction }}"`. From your current location, the directions that you can move to (i.e. they
don't have an object blocking them) are: {{ valid_dirs }}.

Interaction note:
You can only interact (i.e. take actions with) objects that are in your inventory, or directly (i.e.
one square) in front of you, in the direction that you're facing. E.g. if you want to pick an
object up, you need to move directly in front of it, and face it, before using the pick-up action
on it.

Teleportation note:
To make moving easier, you can teleport to a list of specific locations in the environment, using the
teleport action. In this case, 'arg1' is the name of a location. An example teleport action
would be: {"action": "TELEPORT_TO_LOCATION", "arg1": "school"}.

Action Format note:
{{ additional_instructions }}

```

****Required Action Structure**** (no memory or thought fields):

Your response MUST be a single JSON object with keys in this exact order: memory -> thought -> past_data -> hypothesis -> experiment -> (action fields)

**** CRITICAL: INCREMENTAL UPDATE RULE ****

You will see a "Previous State" section showing your last `past_data` and `hypothesis` from the previous step.

- ****ALWAYS start from the previous state and make INCREMENTAL updates****
- ****DO NOT discard previous data or reset known coefficients to null****
- For `past_data`: COPY all previous entries and APPEND new observations (do not recreate from scratch)
- For `hypothesis`: COPY all previous edges/coefficients and UPDATE only what changed based on new evidence
- Only update when there is NEW evidence; otherwise keep the previous values unchanged

1. ****memory**** :a concise but comprehensive running summary that you update EVERY step using (a) your last memory and (b) the most recent few action-observation pairs.
 - Keep memory as complete as possible without being verbose or repeating low-level noise.
 - Include: current subgoal and plan, useful facts discovered, items/locations that matter, pending checks/unknowns, recent failures and why...
 - Do not list raw logs; summarize to help immediately guide the next step.
 - When you observe measurement data, property values, or frequency readings, you should remember them in your memory section"
 - This helps you track patterns, relationships, and make informed decisions"
 - Record key observations such as: crystal properties, frequency measurements, causal relationships you discover, and experimental results"
2. ****thought**** (string): Natural language explanation of why the next action is chosen given current data and hypothesis.
 - Should reference specific gaps in data or hypothesis that motivate the action
 - MUST include accessibility checks: explicitly verify that any UUIDs you reference appear in the interactable objects list or your inventory, and state which list (inventory or interactable)
 - If previous actions failed, explain why they failed and justify why the new action will succeed
 - If transitioning between phases (e.g., property manipulator to reactor), explain the transition logic
3. ****past_data**** (JSON array): Records all available evidence, including baseline, passive observations, and intervention results.
 - Structure: `[{"id": "0/N", "props": {"pH": 95, "Pressure": 103, ...}, "freq": 610}, {"id": "1/N", "props": {"pH": 95, "Pressure": 50, ...}, "freq": 451}, ...]`
 - Each entry MUST include: `id` (experiment counter), `props` (all measured properties as key-value pairs), `freq` (resonance frequency)
 - If available, the first entry (id="0/N") is the baseline before any interventions
 - ****INCREMENTAL UPDATE****: Look at "Last past_data" in Previous State -> COPY ALL existing entries -> APPEND new observations
 - Update rule: APPEND whenever you obtain a new informative observation, whether from passive evidence or from a property-manipulator intervention; keep unchanged during reactor operations unless genuinely new evidence appears there
 - ****DO NOT recreate the array from scratch; always preserve all previous entries****
4. ****hypothesis**** (JSON object): Current understanding of causal structure and frequency relationships.
 - Structure: `{"edges": [{"from": "PropA", "to": "PropB"}, ...], "freq_equation": "resonanceFreq = base + c_PropA*PropA + c_PropB*PropB", "coefficients": {"base": value, "c_PropA": value, "c_PropB": value}}`
 - `edges`: Directed causal relationships between properties (including frequency)
 - `freq_equation`: String representation of hypothesized frequency formula
 - `coefficients`: Numerical values for the equation (use null for unknown coefficients, use real value for known coefficients)
 - ****CRITICAL NAMING CONVENTIONS****:
 - * Coefficient names MUST follow the pattern `c_{property_name}` (e.g., `c_temperatureC`, `c_conductivity`)
 - * ONLY include properties in freq_equation and coefficients that have edges pointing TO the frequency property
 - * DO NOT include coefficients with value 0 (except "base") - if a property doesn't affect frequency, exclude it entirely

```

* Example: If edges show `temperatureC->resonanceFreq` and `conductivity->resonanceFreq`, and
coefficients calculated as c_temperatureC=2 and c_conductivity=1, then:
- freq_equation: `resonanceFreq = base + c_temperatureC*temperatureC + c_conductivity*
conductivity`
- coefficients: `{ "base":20, "c_temperatureC":2, "c_conductivity":1}` (no other properties)
- **INCREMENTAL UPDATE**: Look at "Last hypothesis" in Previous State -> COPY ALL edges/
coefficients -> UPDATE only parts with new evidence
- **PRESERVE known coefficients**: If a coefficient was determined in previous steps, DO NOT reset
it to null unless contradicted
- Update rule: MAY update when new evidence gathered; keep unchanged during reactor operations or
when no new discovery
- **CRITICAL**: Update your frequency equation by REASONING about causal relationships, NOT by
curve-fitting past_data. Do NOT directly fit observation data. Before operating the reactor, your
hypothesis MUST contain a definite frequency equation with all coefficients determined through
causal reasoning.

5. **experiment** (JSON object): Specification of the planned intervention when using the Property
Manipulator, example:
- `{ "target_prop": "PropName", "target_value": number}`
- If no intervention is available or you are not planning one on this step, use `{}` instead of
inventing a fake intervention

6. **Execution action fields** (one of the following):
- Non-dialog actions: `action: "ACTION_NAME", arg1: value, arg2: value` (arg1/arg2 optional
depending on action)
- Dialog option selection: `chosen_dialog_option_int: integer`
- Dialog Value input: `value: number`

**Output Format** (keys in exact order):
```json
{
 "thought": "string explanation",
 "past_data": [array of observation objects],
 "hypothesis": {hypothesis object},
 "experiment": {experiment specification},
 ... action execution fields ...
}
...

Important Guidelines

Causal Discovery Methodology (CRITICAL):
- **Derive frequency equations through CAUSAL REASONING, not data fitting**: Your hypothesis should
be built by understanding which properties causally influence frequency, NOT by curve-fitting
past_data or observation data.
- **Use intervention experiments when available**: When you intervene on property A and observe
changes in property B, this reveals causal relationships. If no interventions are available,
extract as much structure as possible from the passive observations and be explicit about what
remains ambiguous.
- **Before operating the reactor**: Your hypothesis MUST contain a complete frequency equation with
all coefficients determined. Do not leave coefficients as null when transitioning to reactor
operations.
- **For reactor frequency calculation**: Read crystal properties directly from the reactor dialog
text (`dialog_box`).
- **One-way phase transition**: Once you open/talk to the Crystal Reactor, the Property Manipulator
becomes locked and cannot be used again.
- **If a deterministic candidate-graph list is provided in Previous State**: treat it as a hard
consistency filter derived from the configured graph family and the collected data. Use it to
narrow your reasoning, but still explain why the remaining candidates differ.

Data Management:
- `past_data`: Always maintain complete history. When adding passive observations or intervention
results, append to the array (don't replace). During reactor operations, keep past_data unchanged
unless genuinely new evidence appears.

```

- ``hypothesis``: Update edges when causal relationships are discovered or refuted. Update coefficients through causal reasoning from the full evidence set. Keep hypothesis frozen during reactor operations.
- ``thought``: Must explain the logic connecting your current hypothesis/data to the next experiment. If previous actions failed, explain why and justify why the new action will succeed.
- ``experiment``: Must precisely specify what you plan to do next and align with the execution action fields.

**\*\*Example of Incremental Update:\*\***

...

Previous State shows:

```
Last past_data: [{"id":"0/3","props":{"pH":50,"freq":100}]
Last hypothesis: {"edges":[{"from":"pH","to":"resonanceFreq"}],"freq_equation":"resonanceFreq =
base + c_pH*pH","coefficients":{"base":50,"c_pH":1}}
```

After new observation (pH=80, freq=130):

```
[CORRECT] CORRECT: {"past_data":[{"id":"0/3","props":{"pH":50,"freq":100},{"id":"1/3","props":{"pH":80,"freq":130}],
"hypothesis":{"edges":[{"from":"pH","to":"resonanceFreq"}],"freq_equation":"
resonanceFreq = base + c_pH*pH","coefficients":{"base":50,"c_pH":1}}}
[WRONG] WRONG: {"past_data":[{"id":"1/3","props":{"pH":80,"freq":130}],...} // Missing previous
entry!
[WRONG] WRONG: {"hypothesis":{"edges":[],"coefficients":{"base":null,...}}} // Reset known
coefficients!
[WRONG] WRONG: {"freq_equation":"resonanceFreq = base + c1*pH",...} // Wrong coefficient naming!
Should be c_pH
[WRONG] WRONG: {"coefficients":{"base":50,"c_pH":1,"c_pressure":0}} // Don't include zero
coefficients!
...
```

Hints:

- **\*\*CAUSAL REASONING FIRST\*\***: Build your frequency equation by reasoning about causal relationships discovered through interventions, NOT by fitting curves to past\_data. Your equation should reflect the causal structure, not just correlations.
- **\*\*REACTOR DIALOG FIRST\*\***: When calculating target frequency, use the crystal properties shown directly in the reactor dialog.
- **\*\*DO NOT GO BACK\*\***: After entering the reactor phase, do not return to the Property Manipulator. Continue with reactor frequency setting and activation.
- If your last action failed, or other last recent actions failed, please consider thinking why they failed, and trying different actions unless you believe things have changed to make failed actions work this time.
- If you don't see what you're looking for, and anticipate it might be in another location, consider teleporting to that location.
- Use verbose "thought" statements to maintain your progress, running hypotheses, your knowledge about the world, etc. Always include an ACCESSIBILITY CHECK: confirm any UUIDs you reference are from the interactable list/inventory now; otherwise first act to make them accessible.
- REMEMBER, IF YOU'RE GOING TO AN OBJECT, INSTEAD OF MOVING NORTH/EAST/SOUTH/WEST, or ROTATING, YOU SHOULD TRY TELEPORTING DIRECTLY TO OBJECTS. IT'S MUCH FASTER AND LESS ERROR-PRONE. YOU CAN TELEPORT TO AN OBJECT NO MATTER WHERE IT IS, EVEN IF ITS NOT LISTED IN THE ACCESSIBLE OBJECTS LIST. JUST REMEMBER ITS UUID.
- WHEN TELEPORTING, REMEMBER TO LOOK AT THE ENTIRE OBJECT LIST IN THE OBSERVATION, NOT JUST THE ACCESSIBLE OBJECTS LIST.
- FOR ACTIONS INVOLVING TWO ARGS (E.G. USE AND PUT), ONE OF THE OBJECTS MUST BE IN YOUR INVENTORY AND YOU MUST BE NEXT TO THE OTHER OBJECT. E.G. TO USE SHOVEL ON THE SOIL, YOU MUST HAVE THE SHOVEL IN YOUR INVENTORY AND BE NEXT TO THE SOIL.
- IF YOU FIND YOURSELF WAITING FOR SOMETHING TO HAPPEN, CHECK TO SEE IF IT'S ALREADY HAPPENED. YOU MIGHT BE WAITING FOR SOMETHING THAT'S ALREADY HAPPENED.
- IF YOU FIND YOURSELF WAITING FOR A LONG TIME, YOU MIGHT BE STUCK. TRY TO REEXAMINE YOUR TASK, REASSESS WHERE YOU ARE, AND MAKE A NEW PLAN.
- IF YOU THINK YOU ARE DONE, SUBMIT WITH THE ACTION: {"action": "SUBMIT", "arg1": "Task completed!"}.
- IF YOU ARE NOT MAKING ANY PROGRESS AND CAN NOT FIGURE OUT HOW TO PROCEED, USE THE SUBMIT ACTION WITH ARG1 EXPLAINING YOUR REASONING, e.g., {"action": "SUBMIT", "arg1": "Task failed! Unable to explore the building!"}.
- If the target item is nearby but inaccessible, consider ROTATE\_DIRECTION to help yourself face the target item before attempting to move or interact.

```

Task: {{ input_str }}

Current Environment Observation:
```json
{{ observation }}
```

{% if in_dialog %}
NOTE: You are currently in a dialog.
For reference, here is the dialog that you are currently in:
```json
{{ dialog_box }}
```

{% else %}
Valid Actions:
```json
{{ known_actions}}
```

Valid Teleport Locations:
```json
{{ teleport_destinations }}
```

CRITICAL accessibility rules (strict):
- For any `arg1`/`arg2`, choose strictly from the List of objects that are interactable (from your inventory, directly in front of you, or on adjacent tiles north/east/south/west): {{ interactable_objects }}. If an object is not in those lists, first make it accessible (MOVE/ROTATE/TELEPORT/PICK_UP) before acting.
- In your "thought", explicitly state which list you took each UUID from (inventory vs interactable list) and why it is accessible now. If not accessible, state the plan to make it accessible first
.

List of objects that are interactable (from your inventory, and directly in front of you):
{{ interactable_objects }}

{% endif %}

Return ONLY a single JSON object. Keys MUST appear in this exact order: memory -> thought -> past_data -> hypothesis -> experiment -> (action+args OR chosen_dialog_option_int OR value). Do not include any extra text outside the JSON.

```

## Phase 2 Reactor Task Prompt

You are at the Causal Discovery Lab on Planet X. Quantum Crystals have interesting properties that may be causally related.

=== YOUR MISSION ===

THEORETICAL BACKGROUND:

1. CRYSTAL RESONANCE FREQUENCY:
  - Frequency is determined by certain properties (range: 0-100) through LINEAR relationships
  - Frequency CANNOT be directly modified by human intervention
  - Frequency can only change indirectly as a causal consequence of other property changes
2. CAUSAL STRUCTURE:
  - Properties have LINEAR causal relationships with each other
  - These relationships form a DAG (Directed Acyclic Graph):
    - \* No bidirectional influences (if A affects B, B cannot affect A)
    - \* No cycles (no circular chains like A -> B -> C -> A)
    - \* Acyclic structures are allowed (e.g., A -> B, A -> C, B -> D, C -> D)

### 3. PROPERTY INTERVENTION:

- You can intervene on ONE property at a time using the Property Manipulator
- When you modify a property (e.g., prop\_A):
  - \* Other properties CANNOT be simultaneously modified by direct intervention
  - \* However, other properties MAY change automatically as a causal consequence
  - \* Frequency MAY also change if it depends on the modified property or its effects

### 4. MATHEMATICAL MODEL:

- Each property has a BASE VALUE that can be adjusted (except frequency)
- Each property's value = base\_value + sum of causal influences from other properties
- Example: If frequency depends on properties A and B:  

$$\text{frequency} = \text{freq\_base\_value} + k_A * A + k_B * B$$
 (Note: freq\_base\_value is fixed and cannot be adjusted)
- Example: If temperature depends on properties C, D, and E:  

$$\text{temperature} = \text{temp\_base\_value} + k_C * C + k_D * D + k_E * E$$
 (Note: When you adjust temperature, you are actually adjusting temp\_base\_value)
- IMPORTANT: When you modify a property (frequency cannot be directly modified), you are changing its base\_value, which then propagates through the causal graph according to the linear relationships

### CAUSAL DISCOVERY STAGE (If the Property Manipulator is available)

- There is an EXPERIMENT CRYSTAL (quantum crystal 3) currently in the Property Manipulator
- Depending on the experiment setting, you may start with zero or more existing observations and zero or more remaining property adjustments
- If `max_uses` is greater than 0, you may use the Property Manipulator to discover causal relationships
- If `max_uses` is 0, rely on the available observations only and proceed without Property Manipulator interventions
- Goal: Figure out the relationship between controllable and derived properties as far as the available evidence allows

### REACTOR ACTIVATION STAGE

- Once you have extracted all useful information from the available observations/interventions, activate the Crystal Reactor
- Calculate what the crystal's resonance frequency should be based on its properties
- Place the target crystal into the Crystal Reactor
- Set the reactor's frequency to match the crystal's resonance frequency
- Tolerance:  $\pm$  `frequency_tolerance` Hz

### IMPORTANT NOTICE:

- The EXPERIMENT CRYSTAL (used in Phase 1) and the TARGET CRYSTAL (used in Phase 2) are DIFFERENT crystals
- They are not movable between locations
- You CANNOT directly measure the target crystal's frequency - you must calculate it from its properties
- The Property Manipulator shows current crystal properties
- The Property Manipulator has a usage counter showing remaining adjustments

### EXISTING OBSERVATIONS (possibly zero, from previous experiments):

`{ existing_observations }`

### IMPORTANT USAGE INSTRUCTIONS:

- Property Manipulator: Use TALK action, e.g. `{ "action": "TALK", "arg1": <property_manipulator_uuid> }`
  - After dialog opens, the main menu shows available properties to adjust (e.g., Temperature, Moisture, etc.)
  - Step 1: Select the property you want to adjust, e.g., `{ "chosen_dialog_option_int": 1 }` for the first property
  - Step 2: You will enter the value input mode DIRECTLY (no intermediate menu)
  - Step 3: In value input mode, provide ONLY the "value" field in your JSON - do NOT select dialog options
  - Example workflow:
    - \* First TALK: `{ "reasoning": "Selecting property to adjust", "past_data": [...], "hypothesis": {...}, "experiment": {...}, "action": "TALK", "arg1": <uuid>, "chosen_dialog_option_int": 1 }`

```

* Next action: {"reasoning": "Setting property to test hypothesis", "past_data": [...], "
hypothesis": {...}, "experiment": {"target_prop": "PropName", "target_value": 50, "purpose": "..."}, "
value": 50} # Set value (NOT chosen_dialog_option_int!)
- CRITICAL: When in value input mode, you will see "[Do not select this option]" in dialog options
* This is NOT a real option - ignore it!
* Simply provide the "value" field with your desired number
* After setting the value, you automatically return to the main menu
- IMPORTANT: Each property adjustment counts toward your usage limit when interventions are
available.
- Watch the usage counter if it is positive; in some experiment settings it may already be zero.
- CRITICAL: Once you use the Crystal Reactor (set its frequency), you CANNOT use the Property
Manipulator anymore!
- Plan your experiments carefully: use Property Manipulator FIRST, then activate the reactor.

- Crystal Reactor: Use TALK action, e.g. { "action": "TALK", "arg1": <crystal_reactor_uuid> }
- This opens a dialog menu showing the current resonance frequency (range: 0-10,000 Hz)
- Step 1: Select option 1 ("Set frequency to a specific value") to enter frequency input mode
- Step 2: After "is_in_dialog" is True and you are in frequency input mode, include the numeric "
value" field in your JSON with the desired value (0-10000 Hz)
- Example: {..., "chosen_dialog_option_int": 1} to select input mode, then {..., "value": <
frequency_value>} to set frequency
- You can select "Back to main menu" to return to the root menu
- The reactor activates when: (1) target crystal is inside, AND (2) frequency matches crystal's
frequency

```

## A.5. DSL Implementation Details

The DSL hypothesis schema is presented with field-by-field descriptions and a small worked example so the model knows the expected key names, edge format, coefficient format, and convention for referring to frequency. The episode configuration fixes the property names and functional family, so the parser only accepts variables emitted by the environment prompt. If a record fails the schema check, for example because it contains an undeclared property, a non-numeric coefficient, or a mismatch between listed parents and equation terms, we re-prompt up to two times with the parser error before recording a parse failure for that step.

## A.6. Trajectory-Level DSL Visualization

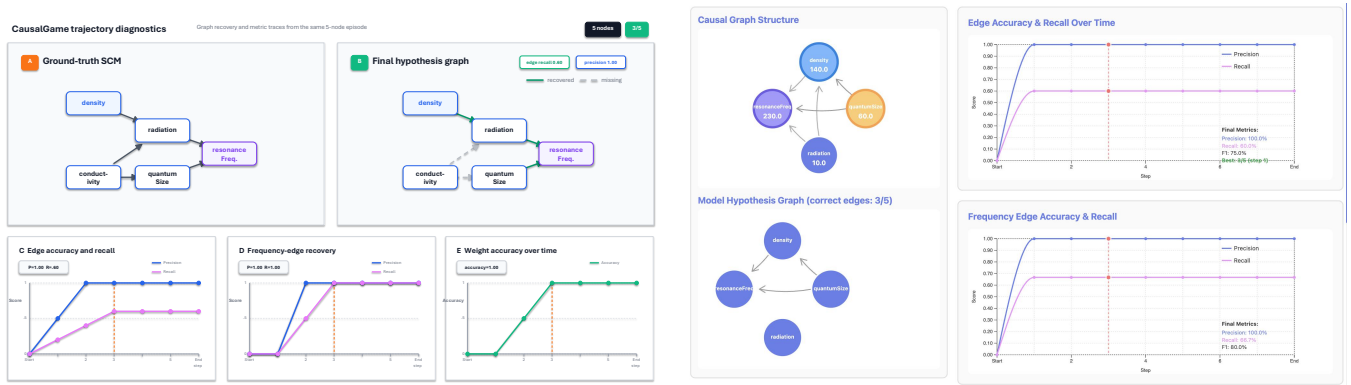
The DSL records make the agent's evolving causal hypothesis auditable, rather than leaving mechanism recovery to be inferred from a final reactor prediction. Figure 8 is included because the DSL and task sections refer to this trajectory-level view: it shows the ground-truth graph, the agent hypothesis graph, and recovery metrics over the interaction sequence.

## A.7. Mechanism Robustness and Perturbation Controls

The main text uses these results to separate task success from causal faithfulness. Table 3 supports the hard-quadratic comparison by showing that the main degradation is in the recovered frequency mechanism, not root discovery. Figure 9 and Table 4 expand the hidden-noise analysis: ordinary hidden count/range perturbations mostly reduce graph  $F_1$ , while perturbing the frequency target family sharply reduces task accuracy. The FreqParent follow-up in Figure 10 and Table 5 tests a related modelling choice: allowing frequency outgoing edges improves prediction but hurts full-graph fidelity.

## A.8. Intervention-Trace Controls

The Golden follow-up tests whether better intervention traces alone are enough to recover a faithful SCM. Table 6 supports the main-text claim that low-MEC traces greatly improve endpoint prediction, yet do not produce matching gains in all-edge recovery.



(a) Paper-ready trajectory schematic.

(b) Visualization-platform screenshot.

**Figure 8:** Trajectory-level causal graph visualizations in *CausaLab*. The schematic and screenshot both expose the ground-truth graph, the agent’s hypothesis graph, and recovery metrics over the intervention sequence.

| Setting                            | Acc. | Root $F_1$ | All-edge P/R/ $F_1$ | Freq-edge $F_1$ | Freq-weight $F_1$ |
|------------------------------------|------|------------|---------------------|-----------------|-------------------|
| GPT-5-mini 4-node linear reference | 48   | 0.559      | 0.833/0.778/0.793   | 0.812           | 0.589             |
| GPT-5-mini 4-node quad-hard        | 24   | 0.829      | 0.902/0.667/0.736   | 0.741           | 0.251             |

Table 3: Linear versus hard-quadratic mechanisms on matched 4-node graphs. The main loss under quadratic dynamics is not root discovery but identifying the correct frequency mechanism.

| Setting                  | Acc. | Root $F_1$ | All-edge P/R/ $F_1$ | Freq-edge $F_1$ | Freq-weight $F_1$ |
|--------------------------|------|------------|---------------------|-----------------|-------------------|
| 4-node main baseline     | 48   | 0.559      | 0.833/0.778/0.793   | 0.812           | 0.589             |
| hidden count = 1         | 50   | 0.708      | 0.854/0.610/0.689   | 0.781           | 0.477             |
| hidden count = 2         | 48   | 0.747      | 0.838/0.576/0.647   | 0.781           | 0.510             |
| hidden count = 3         | 48   | 0.672      | 0.883/0.581/0.671   | 0.799           | 0.493             |
| hidden range = $\pm 0.5$ | 40   | 0.666      | 0.818/0.534/0.614   | 0.729           | 0.389             |
| hidden range = $\pm 5$   | 54   | 0.755      | 0.876/0.610/0.673   | 0.766           | 0.546             |
| hidden range = $\pm 50$  | 52   | 0.675      | 0.920/0.605/0.698   | 0.818           | 0.567             |
| hidden freqnode = 1      | 26   | 0.805      | 0.800/0.573/0.634   | 0.678           | 0.218             |
| hidden freqnode = 2      | 28   | 0.699      | 0.851/0.603/0.670   | 0.735           | 0.327             |
| hidden freqnode = 3      | 40   | 0.623      | 0.850/0.537/0.631   | 0.789           | 0.361             |

Table 4: Hidden-noise robustness on 4-node graphs under exact-context re-evaluation. The table includes the 4-node main baseline, standard hidden settings, and controlled hidden-freqnode settings where resonanceFreq is explicitly included among hidden targets.

### A.9. Model Family and Graph-Size Scaling

These tables give the full numeric support for the model-family and graph-size claims in RQ3. Table 7 combines the 3–7 node GPT and Qwen sweeps behind the model-family radar plots, while Figure 11 shows the corresponding GPT

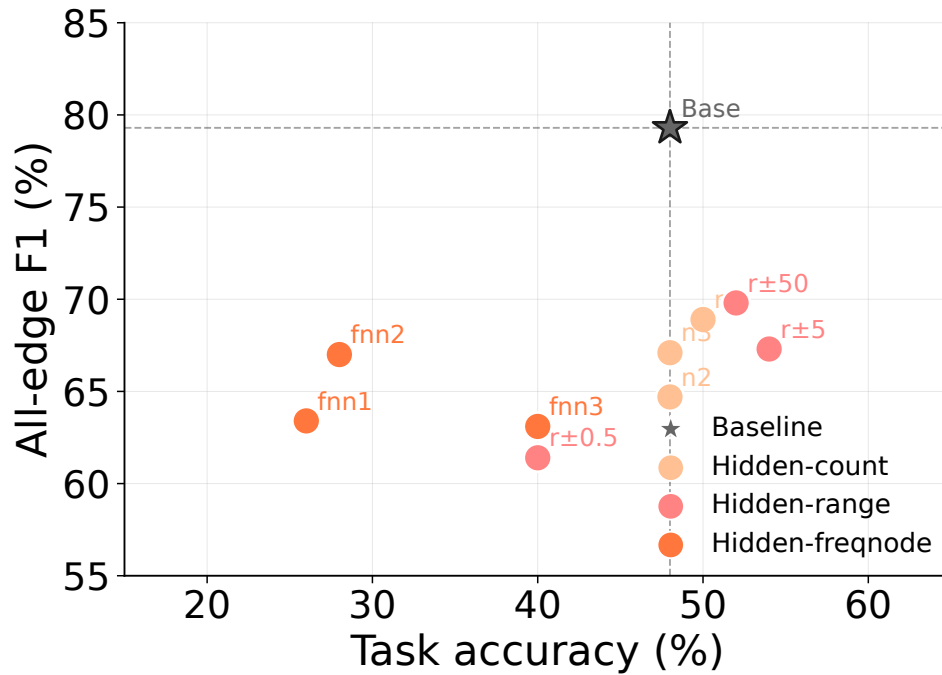


**Figure 9:** Hidden-noise diagnostics across all ten 4-node settings, plotted as (task accuracy, all-edge  $F_1$ ) and colored by noise category. The dashed cross marks the unperturbed baseline. Hidden-count and Hidden-range settings drop  $F_1$  but keep accuracy near baseline; the freqnode family collapses accuracy without further  $F_1$  loss, exposing a fragile parent–target shortcut.

| Suite       | Setting    | $n$ | Acc. | All-edge $F_1$ | Freq-edge $F_1$ | Freq-weight $F_1$ |
|-------------|------------|-----|------|----------------|-----------------|-------------------|
| 4-node main | Baseline   | 50  | 48.0 | 0.793          | 0.812           | 0.589             |
| 4-node main | FreqParent | 50  | 56.0 | 0.606          | 0.733           | 0.451             |
| 6-node main | Baseline   | 50  | 24.0 | 0.628          | 0.679           | 0.455             |
| 6-node main | FreqParent | 50  | 36.0 | 0.387          | 0.582           | 0.364             |

Table 5: FreqParent follow-up under exact-context re-evaluation (GPT-5-mini). Allowing resonanceFreq as a parent improves prediction but degrades full-graph recovery.

absolute metric trajectories (the capability-gap decomposition is in Figure 5 in the main text). Table 8 keeps the small-graph ambiguity diagnostic: even when task accuracy is high, the final hypotheses do not necessarily identify a singleton SCM.

Even on simple 3–4 node settings, high task success does not imply sufficient causal disambiguation: the models’ own interventions leave final IMEC above one, so they do not reduce the possible SCM set to a singleton.

#### A.10. Observation–Intervention Scaling

The scaling appendix supports the RQ2 claim that observations and interventions help different axes of performance. Figure 12 summarizes the regime-level frontier, Figures 13 and 14 show the task and all-edge recovery curves, and Tables 9–12 provide the numeric metric breakdowns for each model/size suite.

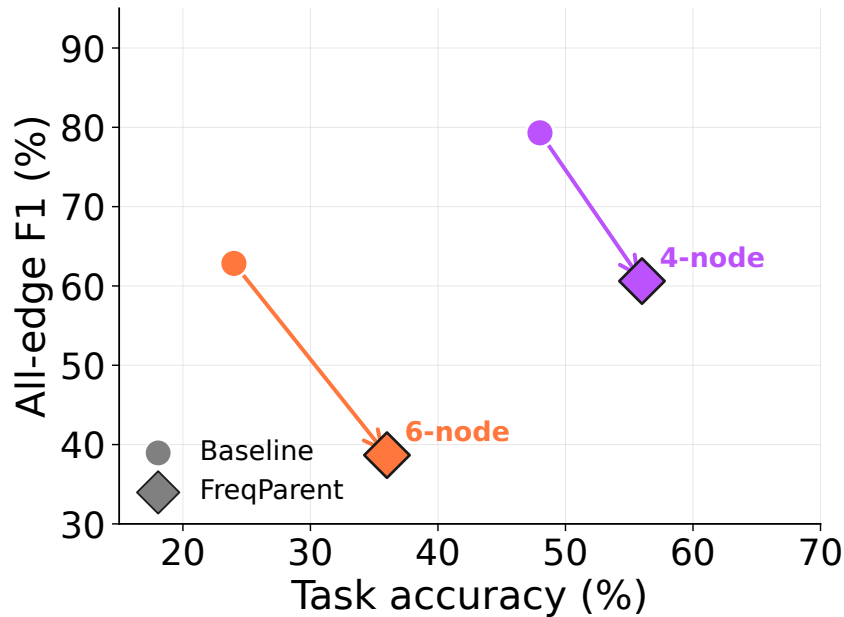


**Figure 10:** FreqParent experiments on GPT-5-mini in (task accuracy, all-edge  $F_1$ ) space. Baseline  $\rightarrow$  FreqParent arrows move down-right on both graph sizes: prediction accuracy rises while graph fidelity falls, especially on 6-node graphs.

| Suite       | Setting  | $n$ | Acc. | All-edge $F_1$ | Freq-edge $F_1$ | Freq-weight $F_1$ |
|-------------|----------|-----|------|----------------|-----------------|-------------------|
| 4-node main | Baseline | 50  | 48.0 | 0.793          | 0.812           | 0.589             |
| 4-node main | Golden   | 50  | 90.0 | 0.728          | 0.743           | 0.644             |
| 6-node main | Baseline | 50  | 24.0 | 0.628          | 0.679           | 0.455             |
| 6-node main | Golden   | 50  | 44.0 | 0.574          | 0.715           | 0.498             |

**Table 6:** Golden follow-up under exact-context re-evaluation (GPT-5-mini). Injected low-MEC intervention traces strongly improve frequency prediction but do not improve all-edge recovery.

The next two tables unpack the GPT-5-mini scaling runs behind the frontier plot. They show the same asymmetry as Figure 12: observation-only budgets often improve endpoint prediction, while mixed observation-intervention budgets are the ones that consistently lift explicit graph recovery.

Figure 13 then plots the same task-prediction axis for both model families and graph sizes, making clear that better endpoint frequency prediction does not by itself certify full causal recovery.

The stronger-model tables below expose the complementary failure mode. Even when GPT-5.2-high solves most endpoint predictions under observation-only budgets, the graph metrics still require mixed interaction.

Finally, Figure 14 plots all-edge recovery directly. The figure is placed after the numeric tables so the reader can first inspect the per-suite values and then compare the aggregate trend across both models.

| Model                | Nodes | Rows | Acc.   | Root $F_1$ | All-edge P/R/ $F_1$ | SHD↓   | Freq-edge $F_1$ | Freq-weight $F_1$ |
|----------------------|-------|------|--------|------------|---------------------|--------|-----------------|-------------------|
| GPT-5-mini           | 3     | 50   | 90.00  | 0.727      | 0.907/0.880/0.889   | 0.458  | 0.907           | 0.890             |
| GPT-5-mini           | 4     | 50   | 48.00  | 0.559      | 0.833/0.778/0.793   | 1.766  | 0.812           | 0.589             |
| GPT-5-mini           | 5     | 50   | 18.00  | 0.413      | 0.825/0.629/0.697   | 3.543  | 0.687           | 0.468             |
| GPT-5-mini           | 6     | 50   | 24.00  | 0.379      | 0.739/0.574/0.628   | 5.490  | 0.679           | 0.455             |
| GPT-5-mini           | 7     | 50   | 16.00  | 0.353      | 0.700/0.449/0.519   | 7.511  | 0.585           | 0.418             |
| GPT-5.2-high         | 3     | 50   | 100.00 | 0.740      | 1.000/1.000/1.000   | 0.000  | 1.000           | 1.000             |
| GPT-5.2-high         | 4     | 50   | 94.00  | 0.590      | 0.957/0.972/0.963   | 0.391  | 0.977           | 0.980             |
| GPT-5.2-high         | 5     | 50   | 92.00  | 0.499      | 0.946/0.896/0.913   | 1.319  | 0.980           | 0.985             |
| GPT-5.2-high         | 6     | 50   | 80.00  | 0.353      | 0.878/0.840/0.838   | 2.660  | 0.956           | 0.956             |
| GPT-5.2-high         | 7     | 50   | 64.00  | 0.273      | 0.855/0.703/0.745   | 4.761  | 0.921           | 0.917             |
| Qwen3.5 non-thinking | 3     | 50   | 72.00  | 0.713      | 0.840/0.717/0.761   | 1.060  | 0.833           | 0.870             |
| Qwen3.5 non-thinking | 4     | 50   | 52.00  | 0.526      | 0.648/0.492/0.539   | 3.520  | 0.640           | 0.691             |
| Qwen3.5 non-thinking | 5     | 50   | 22.00  | 0.551      | 0.727/0.506/0.570   | 4.840  | 0.612           | 0.513             |
| Qwen3.5 non-thinking | 6     | 50   | 20.00  | 0.341      | 0.604/0.374/0.430   | 7.620  | 0.575           | 0.493             |
| Qwen3.5 non-thinking | 7     | 50   | 22.00  | 0.370      | 0.483/0.284/0.331   | 10.800 | 0.497           | 0.508             |
| Qwen3.5 thinking     | 3     | 49   | 95.92  | 0.823      | 0.884/0.745/0.796   | 0.898  | 0.884           | 0.983             |
| Qwen3.5 thinking     | 4     | 50   | 52.00  | 0.663      | 0.711/0.559/0.599   | 3.180  | 0.680           | 0.739             |
| Qwen3.5 thinking     | 5     | 50   | 36.00  | 0.586      | 0.760/0.503/0.578   | 5.040  | 0.717           | 0.614             |
| Qwen3.5 thinking     | 6     | 50   | 34.00  | 0.412      | 0.706/0.403/0.475   | 6.620  | 0.704           | 0.572             |
| Qwen3.5 thinking     | 7     | 50   | 36.00  | 0.463      | 0.609/0.323/0.388   | 9.080  | 0.630           | 0.568             |

Table 7: GPT and Qwen model comparison across the 3–7 node main suites. Acc. is endpoint reactor accuracy in percent; each P/R/ $F_1$  cell reports precision, recall, and  $F_1$  for the corresponding recovery target. SHD is directed all-edge structural Hamming distance, with reversed edges counted as one error.

| Model        | 3-node IMEC | 4-node IMEC |
|--------------|-------------|-------------|
| GPT-5-mini   | 1.920       | 4.540       |
| GPT-5.2-high | 1.480       | 3.620       |

Table 8: Final IMEC on the simple 3- and 4-node main settings.

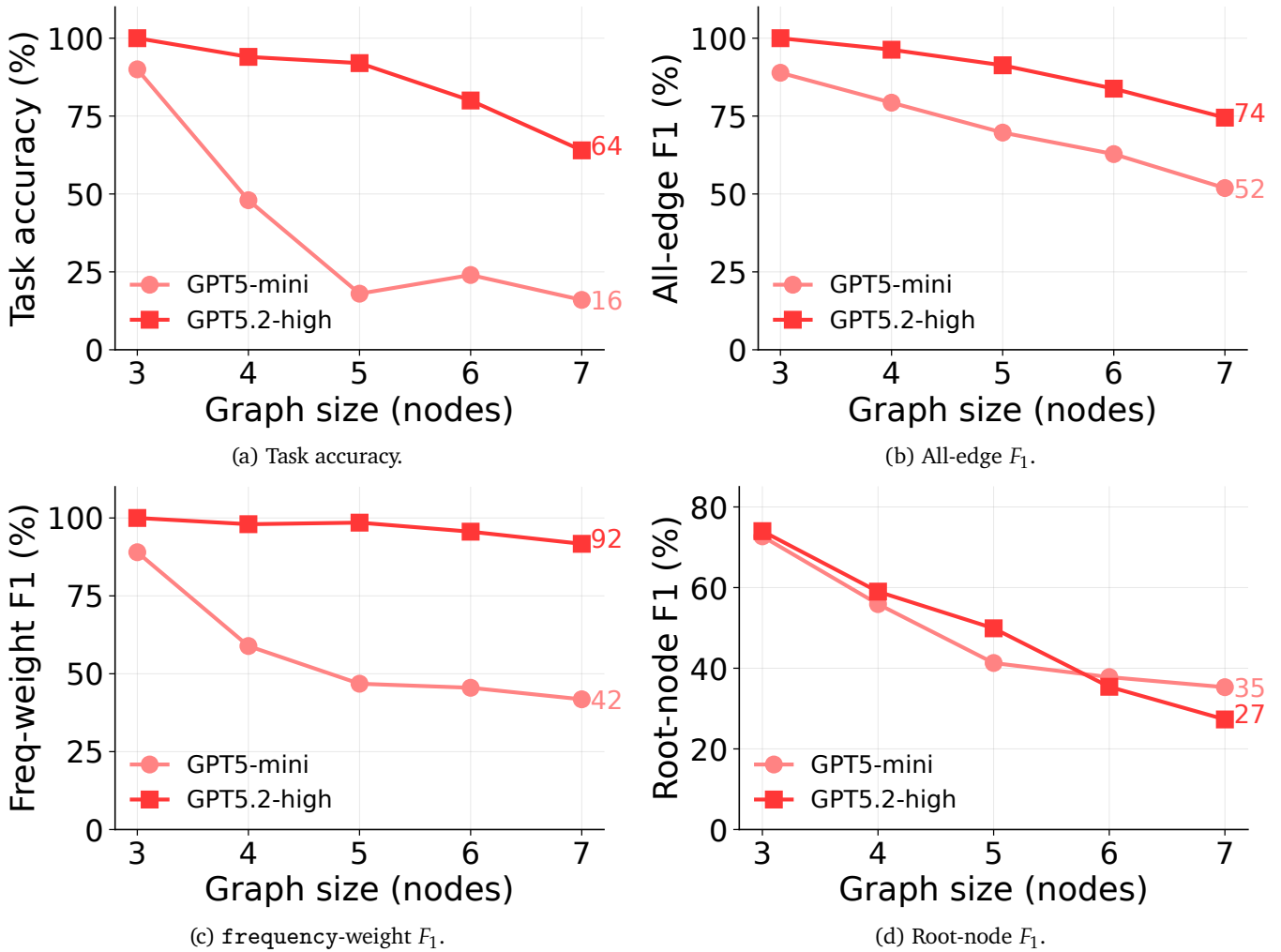


**Figure 11:** Absolute trajectories of the four recovery metrics across graph sizes for GPT-5-mini and GPT-5.2-high. Task accuracy and frequency-weight  $F_1$  separate the two models cleanly; root-node  $F_1$  shows the smallest gap and both models still drop on 6–7 node graphs.

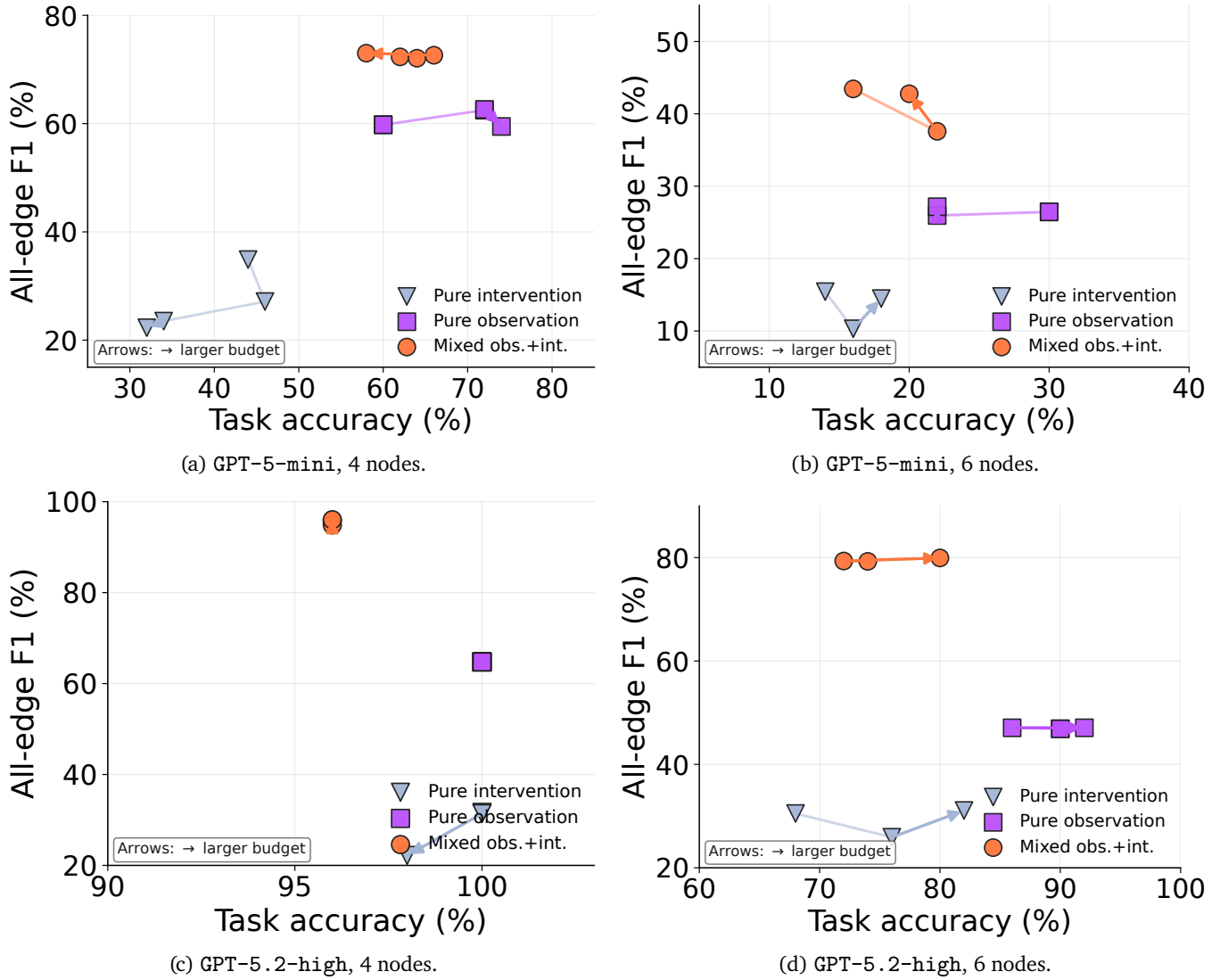


**Figure 12:** All scaling-suite settings plotted as (task accuracy, all-edge  $F_1$ ), colored by regime. Each regime is drawn as a polyline through its settings in order of budget; the arrow on the final segment points toward the largest budget. Mixed obs.+int. reaches the upper part of the frontier; pure observation buys task accuracy without lifting  $F_1$ ; pure intervention stays near the lower-left. The pattern is consistent across both models and both graph sizes.

| Setting                   | Acc. | Root $F_1$ | All-edge P/R/ $F_1$ | Freq-edge $F_1$ | Freq-weight $F_1$ |
|---------------------------|------|------------|---------------------|-----------------|-------------------|
| <i>Pure observation</i>   |      |            |                     |                 |                   |
| 3o0i                      | 60   | 0.542      | 0.905/0.461/0.598   | 0.869           | 0.610             |
| 6o0i                      | 72   | 0.545      | 0.930/0.486/0.625   | 0.901           | 0.727             |
| 12o0i                     | 72   | 0.572      | 0.913/0.489/0.626   | 0.861           | 0.719             |
| 24o0i                     | 74   | 0.542      | 0.898/0.460/0.595   | 0.864           | 0.740             |
| <i>Pure intervention</i>  |      |            |                     |                 |                   |
| 0o3i                      | 44   | 0.315      | 0.416/0.318/0.349   | 0.364           | 0.341             |
| 0o6i                      | 46   | 0.243      | 0.349/0.234/0.271   | 0.318           | 0.315             |
| 0o12i                     | 34   | 0.208      | 0.347/0.194/0.235   | 0.277           | 0.185             |
| 0o24i                     | 32   | 0.213      | 0.300/0.196/0.223   | 0.251           | 0.239             |
| <i>Mixed intervention</i> |      |            |                     |                 |                   |
| 3o0i                      | 60   | 0.542      | 0.905/0.461/0.598   | 0.869           | 0.610             |
| 3o3i                      | 62   | 0.668      | 0.922/0.625/0.723   | 0.839           | 0.729             |
| 3o6i                      | 64   | 0.716      | 0.937/0.616/0.721   | 0.877           | 0.741             |
| 3o12i                     | 66   | 0.719      | 0.922/0.632/0.726   | 0.845           | 0.620             |
| 3o24i                     | 58   | 0.749      | 0.919/0.634/0.730   | 0.843           | 0.609             |

Table 9: GPT-5-mini scaling on 4-node graphs. Rows are grouped into pure observation, pure intervention, and mixed intervention blocks. Task accuracy favors pure observation, while graph-faithfulness favors mixed settings.

| Setting                   | Acc. | Root $F_1$ | All-edge P/R/ $F_1$ | Freq-edge $F_1$ | Freq-weight $F_1$ |
|---------------------------|------|------------|---------------------|-----------------|-------------------|
| <i>Pure observation</i>   |      |            |                     |                 |                   |
| 5o0i                      | 30   | 0.214      | 0.853/0.168/0.265   | 0.622           | 0.310             |
| 10o0i                     | 20   | 0.245      | 0.848/0.165/0.260   | 0.580           | 0.200             |
| 20o0i                     | 14   | 0.271      | 0.812/0.174/0.272   | 0.584           | 0.187             |
| <i>Pure intervention</i>  |      |            |                     |                 |                   |
| 0o5i                      | 12   | 0.095      | 0.298/0.114/0.154   | 0.206           | 0.179             |
| 0o10i                     | 12   | 0.047      | 0.187/0.081/0.103   | 0.142           | 0.110             |
| 0o20i                     | 16   | 0.073      | 0.243/0.108/0.145   | 0.177           | 0.137             |
| <i>Mixed intervention</i> |      |            |                     |                 |                   |
| 5o0i                      | 30   | 0.214      | 0.853/0.168/0.265   | 0.622           | 0.310             |
| 5o5i                      | 26   | 0.378      | 0.868/0.344/0.434   | 0.661           | 0.505             |
| 5o10i                     | 16   | 0.318      | 0.849/0.275/0.376   | 0.590           | 0.409             |
| 5o20i                     | 26   | 0.342      | 0.841/0.320/0.428   | 0.676           | 0.438             |

Table 10: GPT-5-mini scaling on 6-node graphs. Rows are grouped into pure observation, pure intervention, and mixed intervention blocks. Mixed settings improve graph recovery even when all end-task accuracies remain low.

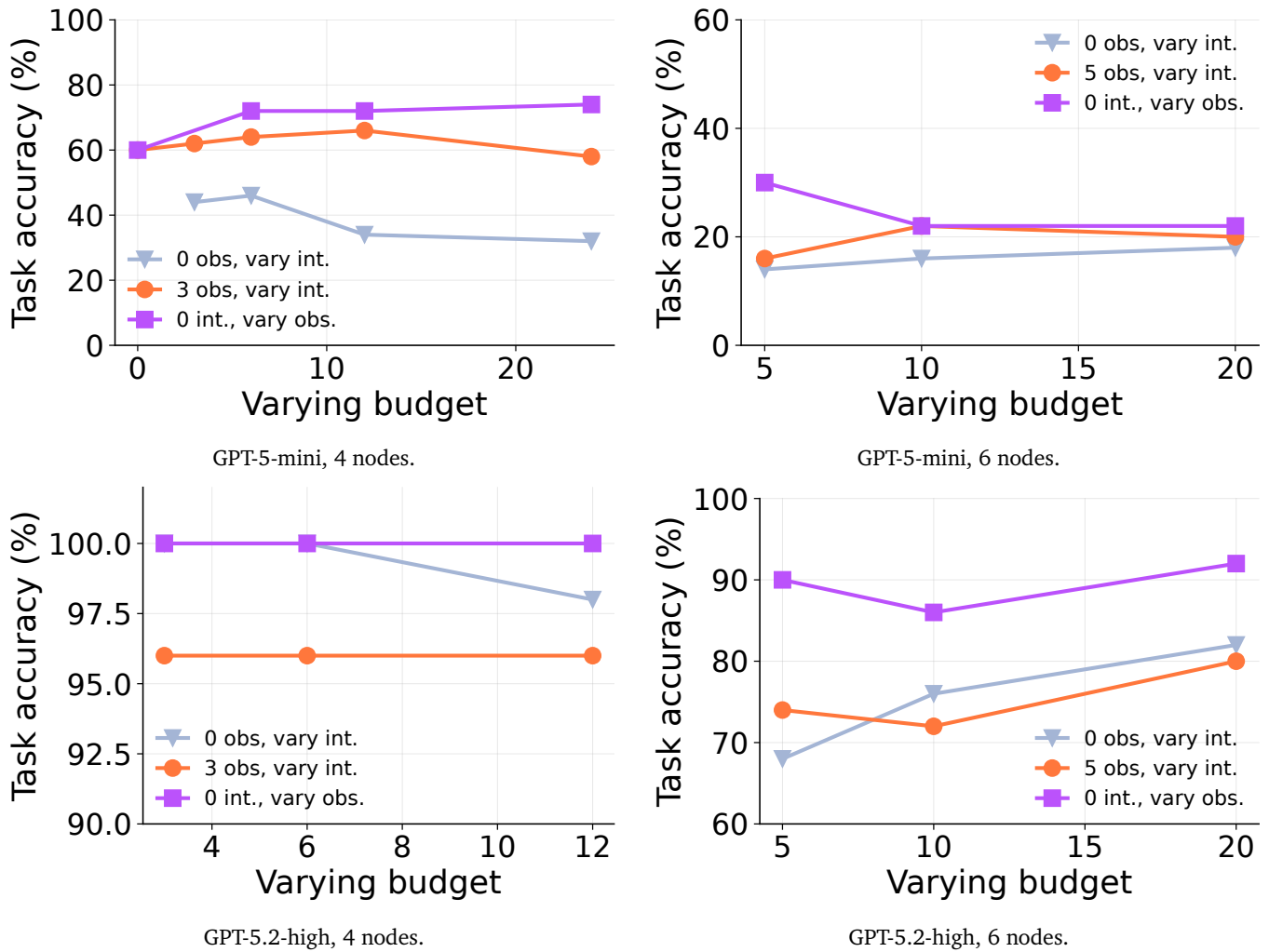


Figure 13: Observation/intervention scaling curves of frequency prediction score under different interaction modes.

| Setting                   | Acc. | Root $F_1$ | All-edge P/R/ $F_1$ | Freq-edge $F_1$ | Freq-weight $F_1$ |
|---------------------------|------|------------|---------------------|-----------------|-------------------|
| <i>Pure observation</i>   |      |            |                     |                 |                   |
| 3o0i                      | 100  | 0.544      | 1.000/0.488/0.648   | 1.000           | 1.000             |
| 6o0i                      | 100  | 0.557      | 1.000/0.488/0.648   | 1.000           | 1.000             |
| 12o0i                     | 100  | 0.541      | 1.000/0.488/0.648   | 1.000           | 1.000             |
| <i>Pure intervention</i>  |      |            |                     |                 |                   |
| 0o3i                      | 100  | 0.330      | 0.310/0.325/0.317   | 0.323           | 0.336             |
| 0o6i                      | 100  | 0.320      | 0.314/0.315/0.314   | 0.330           | 0.348             |
| 0o12i                     | 98   | 0.200      | 0.222/0.223/0.222   | 0.240           | 0.261             |
| <i>Mixed intervention</i> |      |            |                     |                 |                   |
| 3o0i                      | 100  | 0.544      | 1.000/0.488/0.648   | 1.000           | 1.000             |
| 3o3i                      | 96   | 0.947      | 0.971/0.954/0.958   | 0.990           | 0.970             |
| 3o6i                      | 96   | 0.947      | 0.980/0.935/0.949   | 0.987           | 0.987             |
| 3o12i                     | 96   | 0.900      | 0.974/0.956/0.960   | 0.992           | 0.992             |

Table 11: GPT-5.2-high scaling on 4-node graphs. Rows are grouped into pure observation, pure intervention, and mixed intervention blocks. Observation-only settings already solve the reactor task, while mixed settings best recover the full explicit graph.

| Setting                   | Acc. | Root $F_1$ | All-edge P/R/ $F_1$ | Freq-edge $F_1$ | Freq-weight $F_1$ |
|---------------------------|------|------------|---------------------|-----------------|-------------------|
| <i>Pure observation</i>   |      |            |                     |                 |                   |
| 5o0i                      | 90   | 0.309      | 0.990/0.316/0.469   | 1.000           | 1.000             |
| 10o0i                     | 86   | 0.313      | 1.000/0.316/0.471   | 1.000           | 0.980             |
| 20o0i                     | 92   | 0.329      | 1.000/0.316/0.471   | 1.000           | 1.000             |
| <i>Pure intervention</i>  |      |            |                     |                 |                   |
| 0o5i                      | 68   | 0.293      | 0.378/0.278/0.305   | 0.386           | 0.401             |
| 0o10i                     | 76   | 0.130      | 0.278/0.254/0.259   | 0.318           | 0.327             |
| 0o20i                     | 82   | 0.317      | 0.333/0.304/0.311   | 0.379           | 0.385             |
| <i>Mixed intervention</i> |      |            |                     |                 |                   |
| 5o0i                      | 90   | 0.309      | 0.990/0.316/0.469   | 1.000           | 1.000             |
| 5o5i                      | 74   | 0.731      | 0.882/0.763/0.793   | 0.957           | 0.957             |
| 5o10i                     | 72   | 0.687      | 0.874/0.778/0.793   | 0.939           | 0.920             |
| 5o20i                     | 80   | 0.767      | 0.889/0.778/0.799   | 0.957           | 0.959             |

Table 12: GPT-5.2-high scaling on 6-node graphs. Rows are grouped into pure observation, pure intervention, and mixed intervention blocks. Observation-only settings favor end-task success, while mixed settings favor explicit graph recovery.

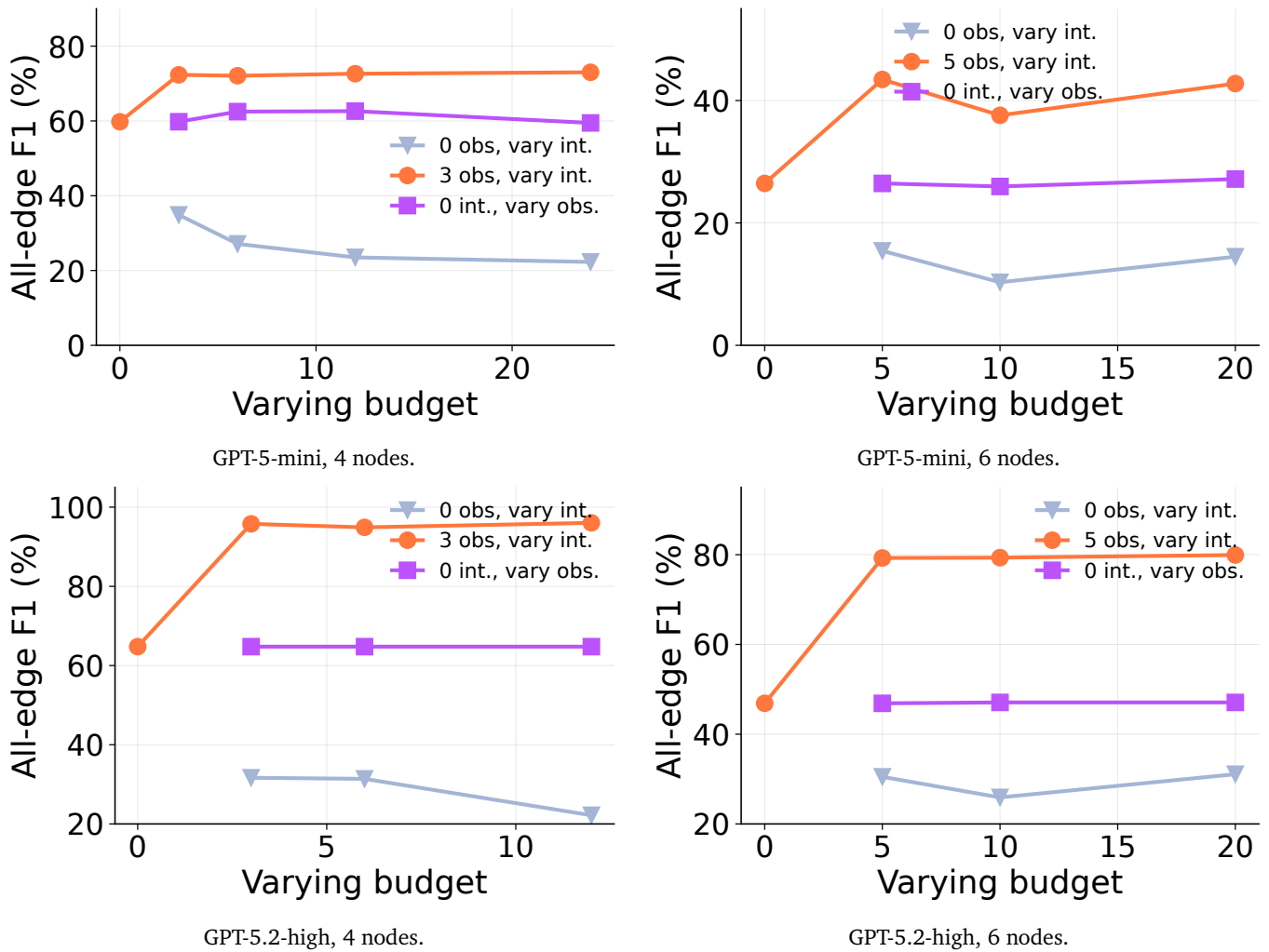


Figure 14: Observation/intervention scaling curves of all-edge recovery  $F_1$  score under different interaction modes.